

This work has been submitted to the *IEEE Journal on Selected Areas in Communications* for possible publication. Copyright may be transferred without notice, after which this version may no longer be accessible.

arXiv:2108.10555v1 [eess.SP] 24 Aug 2021

# MIMO OFDM Dual-Function Radar-Communication Under Error Rate and Beampattern Constraints

Jeremy Johnston, Luca Venturino, *Senior Member, IEEE*, Emanuele Grossi, *Senior Member, IEEE*,  
Marco Lops, *Fellow, IEEE*, Xiaodong Wang, *Fellow, IEEE*

**Abstract**—In this work we consider a multiple-input multiple-output (MIMO) dual-function radar-communication (DFRC) system that employs an orthogonal frequency division multiplexing (OFDM) and a differential phase shift keying (DPSK) modulation, and study the design of the radiated waveforms and of the receive filters employed by the radar and the users. The approach is communication-centric, in the sense that a radar-oriented objective is optimized under constraints on the average transmit power, the power leakage towards specific directions, and the error rate of each user, thus safeguarding the communication quality of service (QoS). We adopt a unified design approach allowing a broad family of radar objectives, including both estimation- and detection-oriented merit functions. We devise a suboptimal solution based on alternating optimization of the involved variables, a convex restriction of the feasible search set, and minorization-maximization, offering a single algorithm for all of the radar merit functions in the considered family. Finally, the performance is inspected through numerical examples.

**Index Terms**—Dual-function radar-communication, orthogonal frequency division multiplexing, multiple-input multiple-output, waveform design, filter design, differential phase shift keying.

## I. INTRODUCTION

The efficient use of the radio spectrum is a long-standing and challenging problem in both the communication and the radar community [1], [2]. The spectrum allocation is regulated by the International Telecommunication Union and periodically revised by the World Radiocommunication Conference. Until recently, the frequency bands assigned to different wireless services have been kept mostly separate to avoid co-channel interference and hence simplify the system design; a static frequency planning, however, is inefficient.

In the recent past, we have witnessed an increasing demand for mobile communication services that has driven the transition across three standards (3/4/5G) and fostered the proliferation of radar-based services in several areas (for

example, industry automation, traffic monitoring, autonomous driving, home surveillance, border patrolling, and earth monitoring); this has raised the cost for using any bandwidth slice and exacerbated the frequency shortage problem [3]. Several solutions to improve the spectral efficiency have been implemented in communication networks, including the use of sophisticated multiple access schemes and of cognitive radios to allow a more dynamic spectrum management [4]–[6], the coordination of adjacent access points to enable a more aggressive spectrum reuse [7]–[9], and the exploitation of the spatial dimension for data encoding, modulation, and multiplexing [10]–[12]. Important technological advances have been also made in the deployment of radar networks [13], opening up the possibility of simultaneously scheduling multiple functions [14] and implementing cognitive systems which sense the environment, learn relevant information, and then adapt to it [15], [16]; also, the use of multiple-input multiple-output (MIMO) digital transceivers [17] and of the waveform diversity [18] have brought novel degrees of freedom for robust target detection [19], [20], adaptive signal processing [21], [22], and reconfigurable beam-pattern design [23], [24].

Cooperative spectrum sharing among licensed radar and communication systems has now established itself as a key enabling technology for efficient exploitation of the available bandwidth. The big divide among the solutions proposed so far is between radar and communication coexistence (RCC), wherein two distinct systems negotiate their transmit/receive strategies in order to control the mutual interference, and dual-functional radar-communication (DFRC) systems, wherein the radar and communication functions are combined in the same hardware platform [25]–[28]. RCC, which resembles the coordinated multi-point transmission/reception in communication or radar networks, mainly results in a multi-objective optimization [29]–[33] involving both radar- and communication-oriented utility functions with separable power constraints; for example, widely-used performance measures are the data rate, the energy efficiency, and the error rate, at the communication side, and the signal-to-interference-plus-noise ratio (SINR), the Cramér Rao bound on the variance of an unbiased estimator of a given unknown parameter, and the mutual information between the received signal and the target response, at the radar side. A DFRC transceiver, conversely, can be implemented by complementing an existing communication module with a full-duplex receiver aimed at detecting the reflections generated by nearby scatterers [34],

J. Johnston and X. Wang are with the Department of Electrical Engineering, Columbia University, New York, NY 10027, United States (e-mail: j.johnston@columbia.edu; xw2008@columbia.edu).

L. Venturino and E. Grossi are with the Department of Electrical and Information Engineering, University of Cassino and Southern Lazio, 03043 Cassino, Italy, and with Consorzio Nazionale Interuniversitario per le Telecomunicazioni, 43124 Parma, Italy (e-mail: l.venturino@unicas.it; e.grossi@unicas.it). The work of L. Venturino and E. Grossi was supported by the research program “Dipartimenti di Eccellenza 2018–2022” sponsored by the Italian Ministry of Education, University, and Research (MIUR).

M. Lops is with the Department of Electrical and Information Technology, University of Naples Federico II, 80138 Naples, Italy, and with Consorzio Nazionale Interuniversitario per le Telecomunicazioni, 43124 Parma, Italy (e-mail: lops@unina.it).

[35], in which case enabling the radar function may require the use of sophisticated receive strategies to cope with the imperfect ambiguity function of the communication signal. Alternatively, a message can be embedded into the waveforms radiated by an existing radar: effective strategies are the use of data-dependent coded pulses in the fast- and slow-time domains, the use of frequency/spatial index modulations, and the control of the sidelobes of the transmit beampattern towards the intended destinations [36]–[41].

#### A. Contribution of the Work

Generally speaking, the joint design of the waveforms emitted by the DFRC transmitter and of the radar and communication receivers is a challenging and still debated problem. The goal of this paper is to make a contribution in this domain; in particular, we consider an DFRC system employing an orthogonal frequency division multiplexing (OFDM) transmission format, wherein a MIMO transceiver simultaneously senses the environment and delivers a message to multiple users. Previous related works on OFDM-DFRC have mainly focused on single-antenna systems where the major degrees of freedom for system design are the joint power allocation and the user scheduling among the available subcarriers [42], [43] and/or the dynamical assignment of one function (either the radar or the communication) to each subcarrier [44]. The corresponding design strategies have consisted in maximizing the achievable communication sum-rate under a constraint on the radar mutual information [42], minimizing the radiated power under constraints on both the radar and the communication mutual information [43], or maximizing the sum of the radar and the communication mutual information [44]. An evolution of [44] is the study presented in [45], addressing the power allocation over a set of subcarriers and symbol intervals so as to maximize the data rate under a similarity constraint safeguarding the radar operation, while accounting for the effect of conveying the control information from the DFRC transceiver to the communication receiver. A massive MIMO system is finally considered in [46], and the many antennas are separated into two groups which radiate the radar and the communication waveforms, respectively: the object of interest is the design of precoders maximizing the communication sum-rate or energy efficiency while maintaining a desired detection performance and a minimum rate per user.

In the context above, the contribution of the present paper can be summarized as follows.

- Since the MIMO structure expands the number of degrees of freedom, both the transmitter and the receiver can be equipped with space-time filters that control the corresponding beampatterns. Here we tackle the joint design of the transmitted waveforms and of the radar and user receivers and formulate a general resource allocation problem wherein the radar performance is optimized under constraints concerning the average transmit power, the transmit beampattern, and the error rate of each user.
- At the radar side, we consider a broad family of merit functions, which includes several estimation- and detection-oriented performance measures: this results in

a unified design approach, which allows the system engineer to reconfigure the radar task at will. For example, the considered family includes the *quasi-arithmetic mean* of the radar SINRs on each subcarrier [47]–[49], the weighted-sum of the *mutual information* between the received signal and the target response on each subcarrier [50]–[54], the weighted-sum of the *Fisher information* for the delay estimation on each subcarrier [55], the weighted-sum of the *detection probability* of the likelihood ratio-test on each subcarrier [56], and the weighted-sum of the two *Kullback-Leibler divergences* between the distributions of the received signal under the null hypothesis and its alternative on each subcarrier [57].

- At the communication side, we do not assume full channel state information (CSI) at the receiver, and a differential phase shift keying (DPSK) modulation is considered: this makes the transmit beampattern independent of the conveyed message and allows the users to employ an incoherent receiver for data demodulation. Needless to say, a coherent phase shift keying (PSK) could be easily accounted for if CSI were available. Also, we include in the model a different statistical characterization of the direct and indirect paths reaching each user.
- Since the considered optimization is not convex, we derive an iterative algorithm—whose structure remains unaltered for all of the radar merit functions in the considered family—to compute a sub-optimal solution, which is based on the alternating optimization of the involved variables, a convex restriction of the feasible search set, and the minorization-maximization algorithm. The proposed procedure monotonically increases the objective function at each iteration and, hence, is convergent.
- Finally, we offer a set of curves showing some achievable radar and communication tradeoffs, as a function of the most relevant system parameters.

#### B. Organization and Notation

The remainder of the paper is organized as follows. In Sec. II, the system description is presented. In Sec. III, the proposed resource allocation problem is formulated and discussed, while a suboptimal solution is derived in Sec. IV. In Sec. V, some examples are given to illustrate the achievable tradeoffs between the radar and the communication operation. Concluding remarks are provided in Sec. VI. Finally, the Appendix contains the proofs of some of the presented results.

In the following,  $\mathbb{R}$ ,  $\mathbb{R}_+$ , and  $\mathbb{C}$  are the set of real, non-negative and real, and complex numbers, respectively, while  $\bar{\mathbb{R}} = \mathbb{R} \cup \{-\infty, \infty\}$  and  $\bar{\mathbb{R}}_+ = \mathbb{R}_+ \cup \{\infty\}$ .  $\mathbb{C}^N$  and  $\mathbb{C}^{N \times N}$  are the set of  $N \times 1$  vectors and  $N \times N$  matrices with complex entries, respectively;  $(\cdot)^T$  and  $(\cdot)^H$  denote transpose and conjugate transpose, respectively;  $\mathbf{I}_N$  is the  $N \times N$  identity matrix;  $\mathbf{1}_N$  and  $\mathbf{0}_N$  are the  $N \times 1$  vectors with all-one and all-zero entries, respectively.  $\text{Tr}\{\mathbf{X}\}$  is the trace of the square matrix  $\mathbf{X}$ ;  $\lambda_{\min}(\mathbf{X})$  and  $\lambda_{\max}(\mathbf{X})$  are the minimum and maximum eigenvalue of the Hermitian matrix  $\mathbf{X}$ , respectively.  $\text{vec}\{\mathbf{X}\}$  is the vector obtained by stacking up the columns of  $\mathbf{X}$ .  $\mathbf{X} \succeq 0$  and  $\mathbf{X} \preceq 0$  means that  $\mathbf{X}$  is Hermitian positive

and negative semidefinite, respectively; if  $\mathbf{X}_1$  and  $\mathbf{X}_2$  are Hermitian matrices, then  $\mathbf{X}_1 \succeq \mathbf{X}_2$  means that  $\mathbf{X}_1 - \mathbf{X}_2 \succeq 0$ .  $\text{diag}(\{x_n\})$  is the diagonal matrix with entries  $x_1, \dots, x_N$ ; we interchangeably use  $f(x_1, \dots, x_N)$ ,  $f(\mathbf{x})$ , and  $f(\{x_n\})$  to denote a function  $f$  of  $\mathbf{x} = (x_1, \dots, x_N)^\top$ .  $f'$ ,  $f''$ , and  $f'''$  are the first, second, and third derivative of  $f$ , respectively.  $C^k$  denotes the differentiability class of order  $k$ .  $f^{-1}$ ,  $\nabla_f$  and  $\nabla_f^2$  are the inverse function, the gradient and the Hessian of  $f$ , respectively.  $\mathbb{1}_{\mathcal{A}}$  is the indicator function of the condition  $\mathcal{A}$ , i.e.,  $\mathbb{1}_{\mathcal{A}} = 1$ , if  $\mathcal{A}$  holds true, and  $\mathbb{1}_{\mathcal{A}} = 0$ , otherwise in the notation paragraph. Finally,  $\otimes$  and  $j$  indicate the Kronecker product and the imaginary unit, respectively.

## II. SYSTEM DESCRIPTION

We consider an OFDM wireless system consisting of a DFRC transmitter, a co-located radar receiver, and  $M$  communication users, each equipped with a linear array with closely-spaced antennas.<sup>1</sup> We denote by  $N_t$ ,  $N_r$ , and  $N_m$  the number of antennas at the transmitter, the radar receiver, and the  $m$ -th user, respectively. The OFDM symbol duration is much longer than the maximum propagation delay, so that a narrowband assumption holds [58]–[60]. A subset of  $K$  subcarriers is employed to simultaneously implement the radar and communication functions, while the other ones are not considered in this work. On each shared subcarrier, the transmitter aims to illuminate the direction of a prospective target while broadcasting a message to the users by using a DPSK modulation [5].

### A. Communication Side

A direct path and/or  $Q_m \geq 0$  indirect paths (produced by as many far-field independent scatterers) can be present between the transmitter and the  $m$ -th user. Accordingly, its discrete-time received signal on the  $k$ -th subcarrier is modeled as

$$y_{k,m} = d_k \underbrace{\left( \beta_{k,m,0} \text{Tr}\{\mathbf{W}_{k,m}^H \mathbf{g}_{k,m}(\bar{\phi}_{m,0}) \mathbf{s}_k^T(\phi_{m,0}) \mathbf{U}_k\} \right)}_{\text{direct link}} + \underbrace{\sum_{q=1}^{Q_m} \beta_{k,m,q} \text{Tr}\{\mathbf{W}_{k,m}^H \mathbf{g}_{k,m}(\bar{\phi}_{m,q}) \mathbf{s}_k^T(\phi_{m,q}) \mathbf{U}_k\}}_{\text{indirect links}} + \text{Tr}\{\mathbf{W}_{k,m}^H \mathbf{Z}_{k,m}\} \quad (1)$$

where:  $\beta_{k,m,0} \in \mathbb{C}$  is the response of the direct path, while  $\bar{\phi}_{m,0}$  and  $\phi_{m,0}$  are the corresponding angles of arrival and departure, respectively;<sup>2</sup>  $\beta_{k,m,q} \in \mathbb{C}$ , for  $q = 1, \dots, Q_m$ , is the response of the  $q$ -th indirect path, while  $\bar{\phi}_{m,q}$  and  $\phi_{m,q}$  are the corresponding angles of arrival and departure, respectively;  $\mathbf{g}_{k,m}(\bar{\varphi}) \in \mathbb{C}^{N_m}$  and  $\mathbf{s}_k(\varphi) \in \mathbb{C}^{N_t}$  are the receive and transmit steering vectors, respectively, which are normalized to have entries with unit magnitude; for example, if a uniform receive array is employed, we have  $\mathbf{g}_{k,m}(\bar{\varphi}) = (1 e^{-j2\pi \frac{f_k b_m}{c} \sin(\bar{\varphi})} \dots e^{-j2\pi \frac{f_k b_m}{c} \sin(\bar{\varphi})(N_m-1)})^\top$ , where  $f_k$  is the center frequency of the  $k$ -th subcarrier,  $b_m$  is the element

spacing, and  $c$  is the speed of light;  $\mathbf{U}_k \in \mathbb{C}^{N_t \times T}$  is the code matrix employed by the transmitter, which spans  $T$  OFDM symbols;  $\mathbf{W}_{k,m} \in \mathbb{C}^{N_m \times T}$  is the filter employed by the user;  $d_k \in \mathcal{D} = \{1, e^{j2\pi/D}, \dots, e^{j2\pi(D-1)/D}\}$  is the DPSK symbol to be broadcast, with  $D$  being the cardinality of the constellation  $\mathcal{D}$ ; and  $\mathbf{Z}_{k,m} \in \mathbb{C}^{N_m \times T}$  is the disturbance vector.

We assume that  $\beta_{k,m,0}$  has a random phase, while its magnitude is deterministic and tied to the pathloss;  $|\beta_{k,m,0}| = 0$  if no direct link is present, while  $|\beta_{k,m,0}| > 0$  otherwise. Also, we consider a Swerling I fluctuation model in each indirect path (as it includes the radar cross-section of the reflecting object), whereby  $\beta_{k,m,q}$  is modeled as a circularly-symmetric Gaussian random variable with variance  $\sigma_{\beta,k,m,q}^2 > 0$  [61]. Finally, we model the entries of  $\mathbf{Z}_{k,m}$  as independent circularly-symmetric Gaussian random variables with variance  $\sigma_{z,k,m}^2 > 0$ .

Upon defining  $\mathbf{u}_k = \text{vec}\{\mathbf{U}_k\}$ ,  $\mathbf{w}_{k,m} = \text{vec}\{\mathbf{W}_{k,m}\}$ ,  $\mathbf{z}_{k,m} = \text{vec}\{\mathbf{Z}_{k,m}\}$ , and  $\mathbf{G}_{k,m}(\bar{\varphi}, \varphi) = \mathbf{I}_T \otimes \mathbf{g}_{k,m}(\bar{\varphi}) \mathbf{s}_k^T(\varphi)$ , the signal in (1) can be recast as

$$y_{k,m} = d_k h_{k,m} + \mathbf{w}_{k,m}^H \mathbf{z}_{k,m} \quad (2)$$

where  $h_{k,m} = \sum_{q=0}^{Q_m} \beta_{k,m,q} \mathbf{w}_{k,m}^H \mathbf{G}_{k,m}(\bar{\phi}_{m,q}, \phi_{m,q}) \mathbf{u}_k$  is the channel response resulting from the superposition of the all paths reaching user  $m$  on subcarrier  $k$ . Notice that  $h_{k,m}$  is a complex random variable, and its magnitude follows a Rice distribution whose scale and shape parameters are [5]

$$\nu_{k,m} = |\beta_{k,m,0}|^2 |\mathbf{w}_{k,m}^H \mathbf{G}_{k,m}(\bar{\phi}_{m,0}, \phi_{m,0}) \mathbf{u}_k|^2 + \sum_{q=1}^{Q_m} \sigma_{\beta,k,m,q}^2 |\mathbf{w}_{k,m}^H \mathbf{G}_{k,m}(\bar{\phi}_{m,q}, \phi_{m,q}) \mathbf{u}_k|^2 \quad (3a)$$

$$\kappa_{k,m} = \frac{|\beta_{k,m,0}|^2 |\mathbf{w}_{k,m}^H \mathbf{G}_{k,m}(\bar{\phi}_{m,0}, \phi_{m,0}) \mathbf{u}_k|^2}{\sum_{q=1}^{Q_m} \sigma_{\beta,k,m,q}^2 |\mathbf{w}_{k,m}^H \mathbf{G}_{k,m}(\bar{\phi}_{m,q}, \phi_{m,q}) \mathbf{u}_k|^2} \quad (3b)$$

respectively. The parameter  $\nu_{k,m} > 0$  is the power received from all paths, while  $\kappa_{k,m} \geq 0$  provides the ratio of the power along the direct path to that along the indirect paths.

Assuming that  $h_{k,m}$  remains constant over two transmissions, we adopt an incoherent receiver to detect the phase offset over consecutive data symbols [5]. We underline that such a receiver does not require the knowledge of  $h_{k,m}$  for data demodulation. For  $D = 2$ , the error probability for the  $m$ -th user on the  $k$ -th subcarrier is [62]

$$E_{k,m} = \frac{1 + \kappa_{k,m}}{2(1 + \kappa_{k,m} + \text{SNR}_{k,m})} \exp\left\{ \frac{-\kappa_{k,m} \text{SNR}_{k,m}}{\kappa_{k,m} + \text{SNR}_{k,m}} \right\} \quad (4)$$

where

$$\text{SNR}_{k,m} = \frac{\nu_{k,m}}{\sigma_{z,k,m}^2 \|\mathbf{w}_{k,m}\|^2} \quad (5)$$

is the signal-to-noise-ratio (SNR). Notice that (4) decreases with both  $\kappa_{k,m}$  and  $\text{SNR}_{k,m}$  (see also [62, Fig. 1]). For  $D > 2$ , an integral expression of the error probability  $E_{k,m}$  is found in [63, Eq. (5)] and omitted here for brevity; while this expression is more cumbersome, it still shows that  $E_{k,m}$  is decreasing with both  $\kappa_{k,m}$  and  $\text{SNR}_{k,m}$ .

<sup>1</sup>The following developments can be also extended to planar arrays.

<sup>2</sup>Hereafter, all angles of arrival/departure are measured with respect to the array broadside direction and are positive when moving clockwise.



### B. Radar Side

The radar inspects the direction  $\psi_k$  on subcarrier  $k$  and is aware of the presence of the self-interference (clutter) produced by  $J \geq 0$  independent scatterers located in the directions  $\theta_1, \dots, \theta_J$  (they can be nearby users or other objects), with  $\theta_j \neq \psi_k$  for any  $j$  and  $k$ . The discrete-time signal received on the  $k$ -th subcarrier is modeled as

$$y_k = \underbrace{d_k \eta_k \text{Tr}\{\mathbf{W}_k^H \mathbf{g}_k(\psi_k) \mathbf{s}_k^T(\psi_k) \mathbf{U}_k\}}_{\text{target}} + \underbrace{d_k \sum_{j=1}^J \alpha_{k,j} \text{Tr}\{\mathbf{W}_k^H \mathbf{g}_k(\theta_j) \mathbf{s}_k^T(\theta_j) \mathbf{U}_k\}}_{\text{clutter}} + \text{Tr}\{\mathbf{W}_k^H \mathbf{Z}_k\} \quad (6)$$

where  $\eta_k \in \mathbb{C}$  is the response of the prospective target,  $\alpha_{k,j} \in \mathbb{C}$  is the response of the  $j$ -th scatterer,  $\mathbf{g}_k(\varphi) \in \mathbb{C}^{N_r}$  is the receive steering vector,  $\mathbf{W}_k \in \mathbb{C}^{N_r \times T}$  is the filter employed by the radar receiver, and  $\mathbf{Z}_k \in \mathbb{C}^{N_r \times T}$  is the disturbance vector.

We assume a Swerling I fluctuation for both the target and the clutter, whereby  $\eta_k$  and  $\alpha_{k,j}$  are independent circularly-symmetric Gaussian variables with variance  $\sigma_{\eta,k}^2 > 0$  and  $\sigma_{\alpha,k,j}^2 > 0$ , respectively [61]; accordingly, the unit-magnitude data symbol  $d_k$  can be absorbed into  $\eta_k$  and  $\alpha_{k,j}$  and does not play any role in the implementation of the radar receiver. Also, the entries of  $\mathbf{Z}_k$  are modeled as independent circularly-symmetric Gaussian variables with variance  $\sigma_{z,k}^2 > 0$ .

Letting  $\mathbf{w}_k = \text{vec}\{\mathbf{W}_k\}$ ,  $\mathbf{z}_k = \text{vec}\{\mathbf{Z}_k\}$ , and  $\mathbf{G}_k(\theta_j) = \mathbf{I}_T \otimes \mathbf{g}_k(\theta_j) \mathbf{s}_k^T(\theta_j)$ , the received signal can be rewritten as

$$y_k = \eta_k \mathbf{w}_k^H \mathbf{G}_k(\psi_k) \mathbf{u}_k + \sum_{j=1}^J \alpha_{k,j} \mathbf{w}_k^H \mathbf{G}_k(\theta_j) \mathbf{u}_k + \mathbf{w}_k^H \mathbf{z}_k \quad (7)$$

and the corresponding SINR is

$$\text{SINR}_k = \frac{\sigma_{\eta,k}^2 |\mathbf{w}_k^H \mathbf{G}_k(\psi_k) \mathbf{u}_k|^2}{\sum_{j=1}^J \sigma_{\alpha,k,j}^2 |\mathbf{w}_k^H \mathbf{G}_k(\theta_j) \mathbf{u}_k|^2 + \sigma_{z,k}^2 \|\mathbf{w}_k\|^2}. \quad (8)$$

We now consider the following family of merit functions for system design

$$f(\text{SINR}_1, \dots, \text{SINR}_K) \quad (9)$$

where  $f: \mathbb{R}_+^K \rightarrow \mathbb{R}_+$  is an increasing function that is either concave or minorized<sup>3</sup> at any point  $\mathbf{x}_0 \in \mathbb{R}_+^K$  by a concave function  $\zeta(\cdot | \mathbf{x}_0)$ .

### C. Transmit Beampattern

The power radiated by the DFRC transmitter towards  $\xi$  on subcarrier  $k$  can be written as

$$\Delta_k(\mathbf{u}_k, \xi) = \frac{1}{T} \|\mathbf{s}_k^T(\xi) \mathbf{U}_k\|^2 = \frac{1}{T} \mathbf{u}_k^H (\mathbf{I}_T \otimes \mathbf{s}_k^*(\xi) \mathbf{s}_k^T(\xi)) \mathbf{u}_k. \quad (10)$$

Notice that  $\Delta_k(\mathbf{u}_k, \xi) \leq N_t \mathcal{P}$ , where  $\mathcal{P}$  is the available power, with equality when all the power is assigned to subcarrier  $k$  (i.e.,  $\mathbf{u}_p = \mathbf{0}_{N_t}$  for  $p \neq k$  and  $\|\mathbf{u}_k\|^2/T = \mathcal{P}$ ) and

<sup>3</sup>The function  $\zeta(\cdot | \mathbf{x}_0)$  minorizes  $f$  at  $\mathbf{x}_0$  if  $f(\mathbf{x}) \geq \zeta(\mathbf{x} | \mathbf{x}_0)$ ,  $\forall \mathbf{x}$ , and  $f(\mathbf{x}_0) = \zeta(\mathbf{x}_0 | \mathbf{x}_0)$  [64].

$\mathbf{u}_k \propto \mathbf{1}_T \otimes \mathbf{s}_k^*(\xi)$ . It is desirable that the transmit beampattern in each subcarrier illuminate the directions corresponding to the prospective target and the connected users, while reducing the power leakage elsewhere, so as to limit the interference possibly caused to the radar receiver and to other co-channel systems operating nearby. We denote by  $\xi_{k,1}, \dots, \xi_{k,L_k}$  the directions to be protected on subcarrier  $k$ , with  $\xi_{k,\ell} \neq \psi_k$ .

### III. PROBLEM FORMULATION

We assume here cognition of the surrounding environment, i.e., that the parameters  $\{\phi_{m,q}, \phi_{m,q}\}$ ,  $\{|\beta_{k,m,0}|\}$ ,  $\{\sigma_{\beta,k,m,q}^2\}$ ,  $\{\sigma_{z,k,m}^2\}$ ,  $\{\theta_j\}$ ,  $\{\sigma_{\alpha,k,j}^2\}$ , and  $\{\sigma_{z,k}^2\}$  can be estimated [15], [16], [26]; on the other hand, the target powers  $\{\sigma_{\eta,k}^2\}$  may be set to a nominal value, as usual in radar design.

For a given  $\mathcal{P}$ , we aim at maximizing a radar merit function of the form in (9), while guaranteeing a desired error rate for each user and constraining the transmit beampattern towards specific directions. The design variables are the transmit code  $\{\mathbf{u}_k\}$ , which allocate the power across the subcarriers and shape the transmit beampattern, and the receiver filters  $\{\mathbf{w}_k, \mathbf{w}_{k,m}\}$ , which provide additional degrees of freedom for interference management. The problem to be solved is

$$\begin{aligned} & \max_{\{\mathbf{u}_k, \mathbf{w}_k, \mathbf{w}_{k,m}\}} f(\{\text{SINR}_k(\mathbf{u}_k, \mathbf{w}_k)\}) \\ \text{s.t. } & \text{C1: } \frac{1}{T} \sum_{k=1}^K \|\mathbf{u}_k\|^2 \leq \mathcal{P} \\ & \text{C2: } \Delta_k(\mathbf{u}_k, \xi_{k,\ell}) \leq \delta_{k,\ell} N_t \mathcal{P}, \quad \forall k, \ell \\ & \text{C3: } E_{k,m}(\mathbf{u}_k, \mathbf{w}_{k,m}) \leq \epsilon_{k,m}, \quad \forall k, m \end{aligned} \quad (11)$$

where  $\delta_{k,\ell} \in [0, 1]$  and  $\epsilon_{k,m} \in (0, 1/2)$ . The above formulation can be readily modified to serve a different set of users on each subcarrier. For example, if user  $m$  only needs to receive the message sent on the first subcarrier, then the constraints on the error probability in the other subcarriers are simply removed; thus an orthogonal frequency division multiple access (OFDMA) can be obtained as a special case.

Problem (11) is non-convex and hence difficult to solve. In the remaining part of this section we provide more insights into Problem (11); then in Section IV we propose a procedure to compute a suboptimal solution.

#### A. Examples of Radar Merit Functions

The family reported in (9) encompasses several relevant merit functions. For example, we can consider the  $p$ -th power mean, with  $p \leq 1$ , of the SINRs on each subcarrier [47]–[49]; in this case we have<sup>4</sup>

$$f(\mathbf{x}) = \left( \sum_{k=1}^K \mu_k x_k^p \right)^{1/p} \quad (12)$$

where  $\{\mu_k\}$  are positive weights with  $\sum_{k=1}^K \mu_k = 1$ . The function in (12) is increasing and its concavity follows from the Minkowski's inequality [48][Ch. 4, Th. 9]. Also, its value becomes more biased towards its smallest argument as  $p$  is

<sup>4</sup>We adopt the convention that  $\frac{1}{0} = \infty$ ,  $\frac{1}{\infty} = 0$ , and  $\alpha + \infty = \infty$  for any  $\alpha \geq 0$ ; accordingly, for  $p < 0$ ,  $f(\mathbf{x}) = 0$  if  $x_k = 0$  for any  $k \in \{1, \dots, K\}$ .

decreased; in particular, it reduces to the arithmetic mean for  $p = 1$ , the geometric mean for  $p \rightarrow 0$ , the harmonic mean for  $p = -1$ , and  $\min_{k \in \{1, \dots, K\}} x_k$  for  $p \rightarrow -\infty$ .

We can also consider the *quasi-arithmetic mean* (also known as *generalized mean*) of the SINRs generated by a continuous strictly monotone function  $\gamma: \mathbb{R}_+ \rightarrow \mathbb{R}$  [47], [48], so that

$$f(\mathbf{x}) = \gamma^{-1} \left( \sum_{k=1}^K \mu_k \gamma(x_k) \right). \quad (13)$$

This function is increasing and subsumes the  $p$ -th power mean for  $\gamma(x) = x^p$  and the Geometric mean for  $\gamma(x) = \ln x$ ; in the other cases, we can prove its concavity by exploiting the following proposition,<sup>5</sup> whose proof is provided in Appendix A.

**Proposition 1.** *Let  $\gamma: \mathbb{R}_+ \rightarrow \mathbb{R}$  be a  $C^4$  function that is either strictly increasing and strictly concave or strictly decreasing and strictly convex. Then  $f(\mathbf{x}) = \gamma^{-1}(\sum_{k=1}^K \mu_k \gamma(x_k))$  is concave if and only if  $\gamma'/\gamma''$  is convex.*

For example,  $\gamma(x) = a^x$ , with  $a \in (0, 1)$ , satisfies the conditions of Proposition 1, so that the resulting *exponential mean* [48], [65]  $f(\mathbf{x}) = \log_a(\sum_{k=1}^K \mu_k a^{x_k})$  is concave. Also,  $\gamma(x) = a^{1/x}$ , with  $a > 1$ , satisfies the conditions of Proposition 1, so that the resulting *radical mean* [48]  $f(\mathbf{x}) = (\log_a(\sum_{k=1}^K \mu_k a^{1/x_k}))^{-1}$  is concave.

Furthermore, we can consider the weighted sum of the *mutual information* between the received signal and the target response on each subcarrier, that is relevant in target classification. In this case, we have [50]–[54]

$$f(\mathbf{x}) = \sum_{k=1}^K \mu_k \ln(1 + x_k) \quad (14)$$

which is increasing and concave.

Additionally, we can consider the weighted-sum of the *Fisher information* for the delay estimation on each subcarrier, which is related to the accuracy in target ranging. In this case, up to an irrelevant scaling factor, we have [55, cfr. Eq. (35)]

$$f(\mathbf{x}) = \sum_{k=1}^K \frac{\mu_k x_k^2}{1 + x_k} \quad (15)$$

which is an increasing function. Moreover, since each term of the summation is convex and, therefore, lower-bounded by the tangent line, we have that  $f$  is minorized at any  $\mathbf{x}_0$  by the following concave (in fact, linear) function

$$\zeta(\mathbf{x}|\mathbf{x}_0) = \sum_{k=1}^K \mu_k \left( \frac{x_{0,k}^2}{1 + x_{0,k}} + \frac{2x_{0,k} + x_{0,k}^2}{(1 + x_{0,k})^2} (x_k - x_{0,k}) \right). \quad (16)$$

Moreover, we can consider the weighted sum of the detection probability of the likelihood ratio-test on each subcarrier. In this case, we have [56]

$$f(\mathbf{x}) = \sum_{k=1}^K \mu_k P_{\text{fa},k}^{1/(1+x_k)} \quad (17)$$

<sup>5</sup>The result of this proposition still holds when the domain of  $\gamma$  is a closed interval  $[a, b] \subseteq \mathbb{R}$ , and the domain of  $f$  is changed accordingly.

where  $P_{\text{fa},k}$  is the probability of false alarm on the  $k$ -th subcarrier. This function is increasing, and, since

$$\left( P_{\text{fa},k}^{1/(1+x_k)} \right)' = - \frac{P_{\text{fa},k}^{1/(1+x_k)} \ln P_{\text{fa},k}}{(1+x_k)^2} \quad (18a)$$

$$\begin{aligned} \left( P_{\text{fa},k}^{1/(1+x_k)} \right)'' &= P_{\text{fa},k}^{1/(1+x_k)} \left( \frac{(\ln P_{\text{fa},k})^2}{(1+x_k)^4} + \frac{2 \ln P_{\text{fa},k}}{(1+x_k)^3} \right) \\ &\geq - \frac{(\sqrt{3}-3)^4 e^{\sqrt{3}-3}}{\sqrt{3} (\ln P_{\text{fa},k})^2} \end{aligned} \quad (18b)$$

a quadratic lower-bound for each term of the summation is readily obtained through Taylor's theorem. Therefore,  $f$  is minorized at any  $\mathbf{x}_0$  by the following concave function

$$\begin{aligned} \zeta(\mathbf{x}|\mathbf{x}_0) &= \sum_{k=1}^K \mu_k \left( P_{\text{fa},k}^{1/(1+x_{0,k})} - \frac{P_{\text{fa},k}^{1/(1+x_{0,k})} \ln P_{\text{fa},k}}{(1+x_{0,k})^2} \right. \\ &\quad \left. \times (x_k - x_{0,k}) - \frac{(\sqrt{3}-3)^4 e^{\sqrt{3}-3}}{2\sqrt{3} (\ln P_{\text{fa},k})^2} (x_k - x_{0,k})^2 \right). \end{aligned} \quad (19)$$

Finally, denote by  $\mathcal{H}_0$  and  $\mathcal{H}_1$  the null hypothesis (i.e., no target is present) and its alternative, respectively. We can consider the weighted-sum of the two *Kullback-Leibler divergences* (or *relative entropies*) between  $\mathcal{H}_0$  and  $\mathcal{H}_1$  and between  $\mathcal{H}_1$  and  $\mathcal{H}_0$  on each subcarrier, that can be used to control the average number of samples needed to make a decision in a sequential probability ratio test with given probabilities of detection and false alarm. In this case, we have [57, cfr. Sec. III]

$$f(\mathbf{x}) = \sum_{k=1}^K \mu_k f_k(x_k) \quad (20)$$

where  $f_k(x_k) = (1 - 2\omega_k) \ln(1 + x_k) + x_k \frac{\omega_k x_k - (1 - 2\omega_k)}{1 + x_k}$ , with  $\omega_k \in [0, 1]$ . This function is increasing, and, since

$$f_k'(x_k) = \frac{x_k(1 + \omega_k x_k)}{(1 + x_k)^2} \quad (21a)$$

$$f_k''(x_k) = \frac{1 - (1 - 2\omega_k)x_k}{(1 + x_k)^3} \geq - \frac{(1 - 2\omega_k)^3}{27(1 - \omega_k)^2} \quad (21b)$$

each term of the summation is convex, if  $\omega_k \geq 1/2$ . Therefore,  $f$  is minorized at any  $\mathbf{x}_0$  by the following concave function

$$\begin{aligned} \zeta(\mathbf{x}|\mathbf{x}_0) &= \sum_{k=1}^K \mu_k \left( f_k(x_{0,k}) + f_k'(x_{0,k})(x_k - x_{0,k}) \right. \\ &\quad \left. - \frac{(1 - 2\omega_k)^3}{54(1 - \omega_k)^2} (x_k - x_{0,k})^2 \mathbb{1}_{\{\omega_k < 1/2\}} \right). \end{aligned} \quad (22)$$

## B. Handling the Error Probability Constraint

Varying  $\mathbf{u}_k$  and/or  $\mathbf{w}_{k,m}$  may have opposite effects on  $\kappa_{k,m}$  and  $\nu_{k,m}$  in (3); accordingly, the best tradeoff in terms of the error probability is in general not simple to assess. Interestingly, the dependency of  $E_{k,m}$  upon  $\mathbf{u}_k$  and  $\mathbf{w}_{k,m}$  simplifies when  $\kappa_{k,m} = \infty$  and  $\kappa_{k,m} = 0$ , as discussed next.

If  $\kappa_{k,m} = \infty$ , then only a direct path is present and no signal fading is observed; in this case, we have

$$E_{k,m} = \frac{1}{2} e^{-\text{SNR}_{k,m}^d} \quad (23)$$

for  $D = 2$ , and<sup>6</sup>

$$E_{k,m} \approx 2Q \left( \sqrt{\text{SNR}_{k,m}^d \sin^2 \frac{\pi}{D}} \right) \quad (24)$$

for  $D > 2$  and  $\text{SNR}_{k,m}^d \gg 1$ , where  $Q(x) = \frac{1}{\sqrt{2\pi}} \int_x^\infty e^{-t^2/2} dt$  and

$$\text{SNR}_{k,m}^d = \frac{|\beta_{k,m,0}|^2 |\mathbf{w}_{k,m}^H \mathbf{G}_{k,m}(\bar{\phi}_{m,0}, \phi_{m,0}) \mathbf{u}_k|^2}{\sigma_{z,k,m}^2 \|\mathbf{w}_{k,m}\|^2}. \quad (25)$$

If  $\kappa_{k,m} = 0$ , then only the indirect paths are present and Rayleigh fading is observed; in this case, we have

$$E_{k,m} = \frac{1}{2(1 + \text{SNR}_{k,m}^i)} \quad (26)$$

for  $D = 2$ , and [66]

$$E_{k,m} \leq \frac{2\pi - \frac{2\pi}{D} + \sin \frac{2\pi}{D}}{2\pi \text{SNR}_{k,m}^i \sin^2 \frac{\pi}{D}} \quad (27)$$

for  $D > 2$ , where

$$\text{SNR}_{k,m}^i = \frac{\sum_{q=1}^{Q_m} \sigma_{\beta,k,m,q}^2 |\mathbf{w}_{k,m}^H \mathbf{G}_{k,m}(\bar{\phi}_{m,q}, \phi_{m,q}) \mathbf{u}_k|^2}{\sigma_{z,k,m}^2 \|\mathbf{w}_{k,m}\|^2}. \quad (28)$$

Remarkably, for any  $\mathbf{u}_k$  and  $\mathbf{w}_{k,m}$ ,  $\kappa_{k,m} = \infty$  if the transmitter and user  $m$  are in the line of sight and no close scatterers are present, while  $\kappa_{k,m} = 0$  if an obstacle blocks the direct path and nearby scatterers redirect the signal emitted by the transmitter towards user  $m$ . In all other cases, we can sub-optimally force  $\kappa_{k,m}$  to be either  $\infty$  or 0 by operating on the transmit and/or receive filters; more specifically, in this study we propose to design  $\mathbf{w}_{k,m}$  to lay either in the null space of the matrices  $\{\mathbf{G}_{k,m}^H(\bar{\phi}_{m,q}, \phi_{m,q})\}_{q=1}^{Q_m}$  or in the null space of  $\mathbf{G}_{k,m}^H(\bar{\phi}_{m,0}, \phi_{m,0})$ , assuming that sufficient degrees of freedom are available (i.e., that  $N_m > Q_m$ ).

If  $\kappa_{k,m} \in \{\infty, 0\}$ , it is verified from (23)–(28) that upper bounding  $E_{k,m}$  amounts to lower bounding

$$\text{SNR}_{k,m} = \begin{cases} \text{SNR}_{k,m}^d, & \text{if } \kappa_{k,m} = \infty \\ \text{SNR}_{k,m}^i, & \text{if } \kappa_{k,m} = 0. \end{cases} \quad (29)$$

Hence, the problem to be solved becomes

$$\begin{aligned} & \max_{\{\mathbf{u}_k, \mathbf{w}_k, \mathbf{w}_{k,m}\}} f(\{\text{SINR}_k(\mathbf{u}_k, \mathbf{w}_k)\}) \\ \text{s.t. C1: } & \frac{1}{T} \sum_{k=1}^K \|\mathbf{u}_k\|^2 \leq \mathcal{P} \\ & \text{C2: } \Delta_k(\mathbf{u}_k, \xi_{k,\ell}) \leq \delta_{k,\ell} N_t \mathcal{P}, \forall k, \ell \\ & \text{C3: } \text{SNR}_{k,m}(\mathbf{u}_k, \mathbf{w}_{k,m}) \geq \rho_{k,m}, \forall m, k \\ & \text{C4: } \mathbf{w}_{k,m} \in \mathcal{W}_{k,m} \end{aligned} \quad (30)$$

where

$$\rho_{k,m} = \begin{cases} \rho_{k,m}^d, & \text{if } \kappa_{k,m} = \infty \\ \rho_{k,m}^i, & \text{if } \kappa_{k,m} = 0 \end{cases} \quad (31)$$

<sup>6</sup>DPSK loses about 3 dB with respect to the coherent PSK at large SNR's, and, in this regime, the nearest neighbor approximation to the error probability of the coherent PSK is tight.

---

### Algorithm 1 Proposed sub-optimal solution to Problem (30)

---

1. Choose  $\eta_{\text{acc}} > 0$ ,  $I_{\text{max}} > 0$ , and  $\{\mathbf{u}_k, \mathbf{w}_k, \mathbf{w}_{k,m}\}$
  2.  $i = 0$  and  $f^{(0)} = f(\{\text{SINR}_k\})$
  3. **repeat**
  4.      $i = i + 1$
  5.     Update  $\{\mathbf{u}_k\}$  by solving (40)
  6.     Update  $\{\mathbf{w}_k\}$  as in (44)
  7.     Update  $\{\mathbf{w}_{k,m}\}$  as explained in Sec. IV-C
  8.      $f^{(i)} = f(\{\text{SINR}_k\})$
  9. **until**  $f^{(i)} - f^{(i-1)} < \eta_{\text{acc}} f^{(i)}$  or  $i = I_{\text{max}}$
- 

is the minimum SNR required to satisfy the error rate constraint for the user  $m$  on subcarrier  $k$  and  $\mathcal{W}_{k,m} = \{\mathbf{w}_{k,m} \in \mathbb{C}^{TN_m} : \kappa_{k,m} \in \{\infty, 0\}\}$ .

Since the feasible search set of Problem (30) is included in that of Problem (11), we have the following result.

**Proposition 2.** *The solution to Problem (30) provides a lower bound to the solution to Problem (11).*

## IV. PROPOSED ALGORITHM

We compute here a suboptimal solution to (30) by resorting to an alternating maximization. Starting from a feasible point, the objective function is maximized with respect to each of the block variables  $\{\mathbf{u}_k\}$ ,  $\{\mathbf{w}_k\}$ , and  $\{\mathbf{w}_{k,m}\}$ , taken in a cyclic order, while keeping the other ones fixed at their previous values. In the following, we discuss in detail the update of each block variable and the selection of the starting point. The overall procedure is summarized in Algorithm 1 and is monotonically convergent, as the value of the objective function is not decreased at each iteration.

### A. Update of the Transmit Code

Upon defining  $\Psi_{k,1} = \sigma_{\eta,k}^2 \mathbf{G}_k^H(\psi_k) \mathbf{w}_k \mathbf{w}_k^H \mathbf{G}_k(\psi_k)$  and  $\Psi_{k,2} = \sum_{j=1}^J \sigma_{\alpha,k,j}^2 \mathbf{G}_k^H(\theta_j) \mathbf{w}_k \mathbf{w}_k^H \mathbf{G}_k(\theta_j)$ , the problem to be solved is

$$\max_{\{\mathbf{u}_k\}} f \left( \left\{ \frac{\mathbf{u}_k^H \Psi_{k,1} \mathbf{u}_k}{\mathbf{u}_k^H \Psi_{k,2} \mathbf{u}_k + \sigma_{z,k}^2 \|\mathbf{w}_k\|^2} \right\} \right), \quad \text{s.t. C1, C2, C3} \quad (32)$$

Notice that the objective function in (32) is non-concave in the optimization variables, while the constraint C3 is non-convex.

To proceed, Problem (32) is first recast as

$$\begin{aligned} & \max_{\{\mathbf{u}_k, x_k\}} f(\mathbf{x}) \\ & \text{s.t. C1, C2, C3} \\ & \text{C5: } \frac{\mathbf{u}_k^H \Psi_{k,1} \mathbf{u}_k}{\mathbf{u}_k^H \Psi_{k,2} \mathbf{u}_k + \sigma_{z,k}^2 \|\mathbf{w}_k\|^2} \geq x_k, \forall k \end{aligned} \quad (33)$$

where  $x_1, \dots, x_K$  are non-negative auxiliary variables and  $\mathbf{x} = (x_1 \cdots x_K)^T$ . Next, a convex restriction of C3 and C5

is derived. Let  $\{\tilde{\mathbf{u}}_k, \tilde{x}_k\}$  be the optimized variables at the previous iteration of Algorithm 1. Then, upon defining

$$\begin{aligned} \mathbf{r}_{k,m} &= \frac{|\beta_{k,m,0}|^2}{\sigma_{z,k,m}^2 \|\mathbf{w}_{k,m}\|^2} \\ &\times \mathbf{G}_{k,m}(\bar{\phi}_{m,0}, \phi_{m,0}) \mathbf{w}_{k,m} \mathbf{w}_{k,m}^H \mathbf{G}_{k,m}^H(\bar{\phi}_{m,0}, \phi_{m,0}) \\ &+ \sum_{q=1}^{Q_m} \frac{\sigma_{\beta,k,m,q}^2}{\sigma_{z,k,m}^2 \|\mathbf{w}_{k,m}\|^2} \\ &\times \mathbf{G}_{k,m}(\bar{\phi}_{m,q}, \phi_{m,q}) \mathbf{w}_{k,m} \mathbf{w}_{k,m}^H \mathbf{G}_{k,m}^H(\bar{\phi}_{m,q}, \phi_{m,q}) \end{aligned} \quad (34)$$

we have [67]

$$\begin{aligned} \text{SNR}_{k,m} &\geq \tilde{\mathbf{u}}_k^H \mathbf{r}_{k,m} \tilde{\mathbf{u}}_k + 2\Re \{ \tilde{\mathbf{u}}_k^H \mathbf{r}_{k,m} (\mathbf{u}_k - \tilde{\mathbf{u}}_k) \} \\ &= 2\Re \{ \tilde{\mathbf{u}}_k^H \mathbf{r}_{k,m} \mathbf{u}_k \} - \tilde{\mathbf{u}}_k^H \mathbf{r}_{k,m} \tilde{\mathbf{u}}_k \end{aligned} \quad (35)$$

where the inequality follows from the fact that  $\text{SNR}_{k,m} = \mathbf{u}_k^H \mathbf{r}_{k,m} \mathbf{u}_k$  is a convex function of  $\mathbf{u}_k$ . At this point, we replace C3 with the following tighter constraint

$$\text{C3R: } 2\Re \{ \tilde{\mathbf{u}}_k^H \mathbf{r}_{k,m} \mathbf{u}_k \} - \tilde{\mathbf{u}}_k^H \mathbf{r}_{k,m} \tilde{\mathbf{u}}_k \geq \rho_{k,m}, \quad \forall m, k. \quad (36)$$

As to C5, first notice that it is active only when  $x_k > 0$ , and, in this case, it can be rewritten as

$$g_k(\mathbf{u}_k, x_k) \geq \mathbf{u}_k^H \Psi_{k,2} \mathbf{u}_k + \sigma_{z,k}^2 \|\mathbf{w}_k\|^2 \quad (37)$$

where  $g_k(\mathbf{u}_k, x_k) = \frac{1}{x_k} \mathbf{u}_k^H \Psi_{k,1} \mathbf{u}_k$ . We now have the following result, whose proof is provided in Appendix B.

**Proposition 3.** Let  $\Psi \in \mathbb{C}^{N \times N}$ , with  $\Psi \succeq 0$ , and  $g(\mathbf{u}, x) = \frac{1}{x} \mathbf{u}^H \Psi \mathbf{u}$ ; then,  $g: \mathbb{C}^N \times (0, \infty) \rightarrow \mathbb{R}$  is convex.

Then, exploiting the convexity of  $g_k$ , we have

$$\begin{aligned} g_k(\mathbf{u}_k, x_k) &\geq g_k(\tilde{\mathbf{u}}_k, \tilde{x}_k) + \Re \left\{ \left( \frac{\partial g_k(\tilde{\mathbf{u}}_k, \tilde{x}_k)}{\partial \mathbf{u}_k} \right)^H \right. \\ &\quad \left. \times (\mathbf{u}_k - \tilde{\mathbf{u}}_k) + \frac{\partial g_k(\tilde{\mathbf{u}}_k, \tilde{x}_k)}{\partial x_k} (x_k - \tilde{x}_k) \right\} \\ &= \frac{2}{\tilde{x}_k} \Re \{ \tilde{\mathbf{u}}_k^H \Psi_{k,1} \mathbf{u}_k \} - \frac{x_k}{\tilde{x}_k^2} \tilde{\mathbf{u}}_k^H \Psi_{k,1} \tilde{\mathbf{u}}_k \end{aligned} \quad (38)$$

if  $\tilde{x}_k > 0$ , where the partial derivatives of  $g_k$  are available from (58a). Therefore, from (37) and (38), we can replace C5 with the following tighter constraint

$$\text{C5R: } \begin{cases} \frac{2}{\tilde{x}_k} \Re \{ \tilde{\mathbf{u}}_k^H \Psi_{k,1} \mathbf{u}_k \} - \frac{x_k}{\tilde{x}_k^2} \tilde{\mathbf{u}}_k^H \Psi_{k,1} \tilde{\mathbf{u}}_k \\ \geq \mathbf{u}_k^H \Psi_{k,2} \mathbf{u}_k + \sigma_{z,k}^2 \|\mathbf{w}_k\|^2, & \forall k: \tilde{x}_k > 0 \\ x_k = 0, & \forall k: \tilde{x}_k = 0. \end{cases} \quad (39)$$

We now propose to solve the following restricted problem

$$\max_{\{\mathbf{u}_k, x_k\}} f(\mathbf{x}), \quad \text{s.t. C1, C2, C3R, C5R.} \quad (40)$$

If  $f$  is concave, then (40) is a convex problem and can be solved by using standard optimization techniques [67]; in this case, a solution to (40) is also a feasible point for (32); also, after updating  $\{\mathbf{u}_k, x_k\}$  as in (40), the value of the objective function in (32) is not decreased.

If  $f$  is minorized at any point by a concave function, we can sub-optimally solve Problem (40) via a minorization-maximization algorithm [64]. Specifically, starting from  $\mathbf{x}^{(0)} = (\tilde{x}_1, \dots, \tilde{x}_K)^T$ , a sequence of feasible points is generated by the following induction: given  $\mathbf{x}^{(i-1)}$ , choose  $\mathbf{x}^{(i)}$  as the solution to the following convex problem

$$\max_{\{\mathbf{u}_k, x_k\}} \zeta(\mathbf{x} | \mathbf{x}^{(i-1)}), \quad \text{s.t. C1, C2, C3R, C5R.} \quad (41)$$

The solution to (41) is a feasible point for (32); also, after updating  $\{\mathbf{u}_k, x_k\}$  as in (41), we have

$$f(\mathbf{x}^{(i)}) \geq \zeta(\mathbf{x}^{(i)} | \mathbf{x}^{(i-1)}) \geq \zeta(\mathbf{x}^{(i-1)} | \mathbf{x}^{(i-1)}) = f(\mathbf{x}^{(i-1)}) \quad (42)$$

whereby  $\{f(\mathbf{x}^{(i)})\}_{i \in \mathbb{N}}$  is a non decreasing sequence. Since solving (40) is part of an alternating-maximization algorithm, it is not necessary to iterate the maximization of  $g(\mathbf{x} | \mathbf{x}^{(i-1)})$  in (41) until convergence and we can just proceed to update the other block variables  $\{\mathbf{w}_k\}$  and  $\{\mathbf{w}_{k,m}\}$  after only one or few steps of inner minorization-maximization.

### B. Update of the Radar Receive Filters

The filter  $\mathbf{w}_k$  only comes into play in the objective function. Since  $f$  is increasing, the optimal  $\mathbf{w}_k$  must maximize  $\text{SINR}_k$ . This problem is separable for each user and subcarrier and admits a closed form solution. Indeed, we have

$$\begin{aligned} \text{SINR}_k &= \frac{\sigma_{\eta,k}^2 \mathbf{w}_k^H \mathbf{G}_k(\psi_k) \mathbf{u}_k \mathbf{u}_k^H \mathbf{G}_k(\psi_k) \mathbf{w}_k}{\mathbf{w}_k^H \Phi_k(\mathbf{u}_k) \mathbf{w}_k} \\ &\leq \sigma_{\eta,k}^2 \mathbf{u}_k^H \mathbf{G}_k^H(\psi_k) \Phi_k^{-1}(\mathbf{u}_k) \mathbf{G}_k(\psi_k) \mathbf{u}_k \end{aligned} \quad (43)$$

where  $\Phi_k(\mathbf{u}_k) = \sum_{j=1}^J \sigma_{\alpha,k,j}^2 \mathbf{G}_k(\theta_j) \mathbf{u}_k \mathbf{u}_k^H \mathbf{G}_k(\theta_j) + \sigma_{z,k}^2 \mathbf{I}_{N_r}$ , and the upper bound is achieved (up to an irrelevant scaling factor) when

$$\mathbf{w}_k = \Phi_k^{-1}(\mathbf{u}_k) \mathbf{G}_k(\psi_k) \mathbf{u}_k. \quad (44)$$

### C. Update of the User Receive Filters

Let  $\Pi_{k,m}^d$  be equal to the projector onto the orthogonal complement of the subspace spanned by the vectors  $\{\mathbf{g}_{k,m}(\bar{\phi}_{m,q})\}_{q=1}^{Q_m}$ , if  $Q_m > 0$ , and to  $\mathbf{I}_{N_m}$  otherwise; also, let  $\Pi_{k,m}^i$  be equal to the projector onto the orthogonal complement of the subspace spanned by  $\mathbf{g}_{k,m}(\bar{\phi}_{m,0})$ , if  $|\beta_{k,m,0}| > 0$ , and to  $\mathbf{I}_{N_m}$  otherwise; finally, let

$$\begin{aligned} \Xi_{k,m} &= \frac{|\beta_{k,m,0}|^2}{\sigma_{z,k,m}^2} \mathbf{G}_{k,m}(\bar{\phi}_{m,0}, \phi_{m,0}) \mathbf{u}_k \mathbf{u}_k^H \mathbf{G}_{k,m}^H(\bar{\phi}_{m,0}, \phi_{m,0}) \\ &+ \sum_{q=1}^{Q_m} \frac{\sigma_{\beta,k,m,q}^2}{\sigma_{z,k,m}^2} \mathbf{G}_{k,m}(\bar{\phi}_{m,q}, \phi_{m,q}) \mathbf{u}_k \mathbf{u}_k^H \mathbf{G}_{k,m}^H(\bar{\phi}_{m,q}, \phi_{m,q}). \end{aligned} \quad (45)$$

Then, we have the following result, whose proof is reported in Appendix C.

**Proposition 4.** If Problem (30) is feasible, then the optimal  $\mathbf{w}_{k,m}$  is proportional to the eigenvector corresponding to the largest eigenvalue of  $\Xi_{k,m}^d = (\mathbf{I}_T \otimes \Pi_{k,m}^d) \Xi_{k,m} (\mathbf{I}_T \otimes \Pi_{k,m}^d)$ , if  $\kappa_{k,m} = \infty$ , and of  $\Xi_{k,m}^i = (\mathbf{I}_T \otimes \Pi_{k,m}^i) \Xi_{k,m} (\mathbf{I}_T \otimes \Pi_{k,m}^i)$ , if  $\kappa_{k,m} = 0$ , for  $m = 1, \dots, M$  and  $k = 1, \dots, K$ .



According to Proposition 4, the filter  $\mathbf{w}_{k,m}$  has to be chosen equal to the eigenvector corresponding to the maximum eigenvalue of either  $\Xi_{k,m}^d$  or  $\Xi_{k,m}^i$ . When both these solutions are feasible, we select the one providing the lower error probability; otherwise, we select the only one feasible.

Notice in passing that, by leveraging Proposition 4, we can also obtain the following side result on the feasibility of C3, whose proof is reported in Appendix D.

**Proposition 5.** *A necessary condition for the feasibility of C3 in Problem (30) is  $\|\mathbf{U}_k^H \mathbf{s}_k^*(\phi_{m,0})\| \neq 0$ , if  $\kappa_{k,m} = \infty$ , and  $\max_{q \in \{1, \dots, Q_m\}} \|\mathbf{U}_k^H \mathbf{s}_k^*(\phi_{m,q})\| > 0$ , if  $\kappa_{k,m} = 0$ , for  $m = 1, \dots, M$  and  $k = 1, \dots, K$ . If  $\text{Rank}\{\mathbf{U}_k\} = N_t$ , a sufficient condition for the feasibility of C3 in Problem (30) is*

$$\lambda_{\min}(\mathbf{U}_k \mathbf{U}_k^H) \geq \begin{cases} \frac{\rho_{k,m}^d \sigma_{z,k,m}^2 / N_t}{|\beta_{k,m,0}|^2 \mathbf{g}^H(\bar{\phi}_{m,0}) \mathbf{\Pi}_{k,m}^d \mathbf{g}_{k,m}(\bar{\phi}_{m,0})}, & \text{if } \kappa_{k,m} = \infty \\ \frac{\rho_{k,m}^i \sigma_{z,k,m}^2 / N_t}{\max_q |\beta_{k,m,q}|^2 \mathbf{g}^H(\bar{\phi}_{m,q}) \mathbf{\Pi}_{k,m}^i \mathbf{g}_{k,m}(\bar{\phi}_{m,q})}, & \text{if } \kappa_{k,m} = 0 \end{cases} \quad (46)$$

for  $m = 1, \dots, M$  and  $k = 1, \dots, K$ .

#### D. Selection of the Starting Point

Next we outline a possible method to obtain a starting point for Algorithm 1. To this end, consider the following problem

$$\begin{aligned} & \max_{t, \{\mathbf{u}_k\}, \{\mathbf{w}_{k,m}\}} t \\ & \text{s.t. C1, C2, C4} \\ & \overline{\text{C3}}: \text{SNR}_{k,m}(\mathbf{u}_k, \mathbf{w}_{k,m}) / \rho_{k,m} \geq t. \end{aligned} \quad (47)$$

If the optimal  $t$  is not lower than 1, then the corresponding variables  $\{\mathbf{u}_k\}$  and  $\{\mathbf{w}_{k,m}\}$  together with the radar receive filters  $\{\mathbf{w}_k\}$  obtained as by-product from (44) are a feasible point for Algorithm 1. Since (47) is an NP-hard program [68], we resort here to an alternating maximization of the block variables  $\{t, \mathbf{u}_k\}$  and  $\{\mathbf{w}_{k,m}\}$ . Given  $\{\mathbf{w}_{k,m}\}$ , we can update  $\{t, \mathbf{u}_k\}$  by solving the following problem

$$\max_{t, \{\mathbf{u}_k\}} t, \quad \text{s.t. C1, C2, } \overline{\text{C3}}, \quad (48)$$

which can be tackled, similarly to what was done for Problem (33), by introducing a convex restriction of  $\overline{\text{C3}}$ . Also, given  $\{t, \mathbf{u}_k\}$ , we can update  $\{\mathbf{w}_{k,m}\}$  as described in Sec. IV-C. At the beginning,  $\{\mathbf{u}_k\}$  can be randomly selected and normalized to meet C1. Also,  $\{\mathbf{w}_{k,m}\}$  can be initialized as follows. First we randomly decide whether user  $k$  will utilize the direct path or the indirect paths (if both present) on the  $k$ -th subcarrier; if the direct path is used, then  $\mathbf{w}_{k,m} = (\mathbf{I}_T \otimes \mathbf{\Pi}_{k,m}^d)(\mathbf{I}_T \otimes \mathbf{g}_{k,m}(\bar{\phi}_{m,0}))$ , otherwise,  $\mathbf{w}_{k,m} = (\mathbf{I}_T \otimes \mathbf{\Pi}_{k,m}^i)(\mathbf{I}_T \otimes \mathbf{g}_{k,m}(\bar{\phi}_{m,\hat{q}}))$ , where  $\hat{q} = \max_{q \in \{1, \dots, Q_m\}} \sigma_{\beta,k,m,q}^2$ .

Next we outline a method to obtain a starting point for Algorithm 1. Initial  $\{\tilde{\omega}_k\}$  may be chosen arbitrarily small in order to satisfy (39), while  $\{\mathbf{u}_k\}$  and  $\{\mathbf{w}_{k,m}\}$  may be found as follows. Our approach is to attempt to solve

Table I

Parameter	Value	Description
$N_t$	11	number of transmit antennas
$N_r$	4	number of radar receive antennas
$N_c$	4	number of user receive antennas
$K$	4	number of subcarriers
$T$	2	number of time slots
$J$	4	number of clutter objects
$D$	2	constellation size

## V. NUMERICAL ANALYSIS

We consider an OFDM system using a power  $\mathcal{P} = 20$  dBW on the shared subcarriers; also, the center frequency of the subcarriers is  $f_k = f_0 + (k - 1)\Delta f$ , for  $k = 1, \dots, K$ , where  $f_0 = 2$  GHz and  $\Delta f = 100$  KHz. Each array has a uniform element spacing of  $c/(2 \max_k f_k)$ , while all angles of arrival/departure are sampled from the uniform distribution on  $[-\pi/3, \pi/3]$ . At the communication side, we set  $\epsilon_{k,m} = \epsilon$  and  $\sigma_{z,k,m}^2 = -150$  dBW; also, the connected users will have either one direct path or two indirect paths—they will be referred to as the direct and indirect users, respectively. The response of the direct path is set to have  $|\beta_{k,m,0}|^2 = -130$  dB, while that of the indirect paths is chosen to have  $\sum_{q=1}^{Q_m} \sigma_{\beta,k,m,q}^2 = -130$  dB. At the radar side, we set  $\delta_{k,\ell} = \delta$ ,  $L_k = L$ ,  $\sigma_{z,k}^2 = -150$  dBW, and  $\sigma_{\eta,k}^2 = -160$  dB, while the clutter power is assumed equal for all scatterers and adjusted according to a given signal-to-clutter ratio (SCR), defined as  $\text{SCR} = \sigma_{\eta,k}^2 / \sum_{j=1}^J \sigma_{\alpha,k,j}^2$ . Unless otherwise stated, we assume two direct and two indirect users (whereby  $M = 4$ ),  $L = 6$  protected directions with  $\delta = 10^{-6}$ , an error rate of  $\epsilon = 10^{-5}$ , and an SCR of  $-20$  dB. The remaining system parameters are reported in Table I.

In the following, we focus on the arithmetic mean of the radar SINRs on each subcarrier, i.e., the merit function in (12) with  $p = 1$ , and on the weighted-sum of the Kullback-Leibler divergence between the distributions of the received signal under  $\mathcal{H}_0$  and  $\mathcal{H}_1$  on each subcarrier, i.e., the merit function in (20) with  $\omega_k = 0$  for  $k = 1, \dots, K$ ; in both cases, we set  $\mu_k = 1/K$  for  $k = 1, \dots, K$ . Algorithm 1 is implemented with  $\eta_{\text{acc}} = 10^{-4}$  and  $I_{\text{max}} = 2000$ . The block variables  $\{\mathbf{u}_k\}$ ,  $\{\mathbf{v}_k\}$ , and  $\{\mathbf{w}_{k,m}\}$  are initialized as in Sec IV-D, and finally the auxiliary variable  $\tilde{x}_k$  in Problem (40) is initialized to the initial  $\text{SINR}_k$ , for  $k = 1, \dots, K$ .

#### A. Examples

First we examine the system tradeoffs as a function of  $\epsilon$  and  $\delta$ . In the top plot of Fig. 1, we report the arithmetic mean of the radar SINRs provided by Algorithm 1 versus  $\epsilon$  for  $\delta = 10^{-6}, 10^{-3}, 1$ ; two SCRs are considered, namely,  $-20$  dB (solid) or  $20$  dB (dashed). The reported curves are obtained by averaging over 10 feasible problem instances. Not surprisingly, a lower objective is attained when  $\delta$  and/or SCR decrease, since the system consumes more degrees of freedom to reduce the power leakage towards the clutter and the protected directions; notice here that  $\delta = 1$  is tantamount to removing C2. Also, when  $\epsilon$  gets larger than  $10^{-3}$ , the communication function no longer restrains the radar. Finally, in

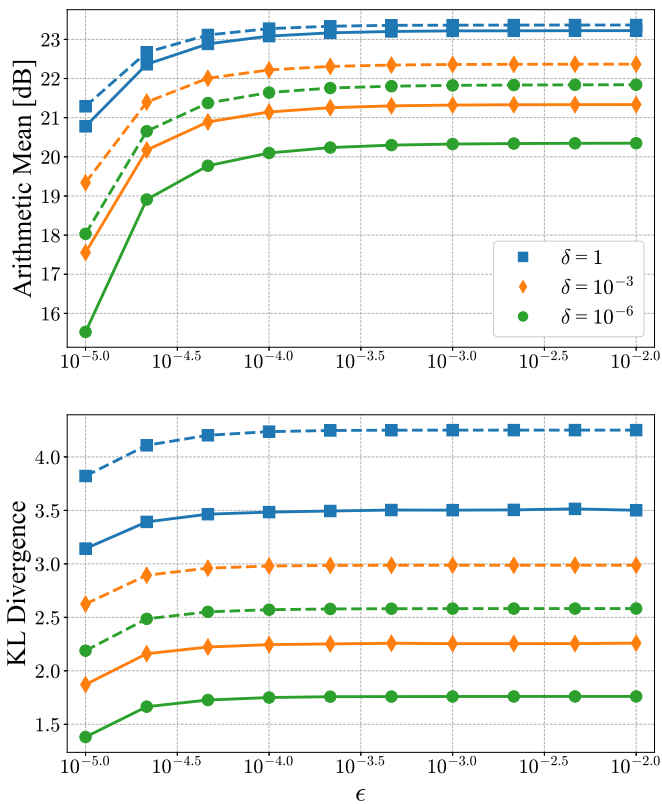


Figure 1. Arithmetic mean of the radar SINRs (top) and weighted-sum of the Kullback-Leibler divergence between the distributions of the received signal under  $\mathcal{H}_0$  and  $\mathcal{H}_1$  (bottom) vs  $\epsilon$  for  $\delta = 10^{-6}, 10^{-3}, 1$ . The solid and dashed lines correspond to an SCR of  $-20$  dB and  $20$  dB, respectively.

the bottom plot of Fig. 1, we also report the weighted-sum of the Kullback-Leibler divergence between the distributions of the received signal under  $\mathcal{H}_0$  and  $\mathcal{H}_1$  provided by Algorithm 1, under the same system setup considered above: it is seen that similar tradeoffs in terms of SCR,  $\epsilon$ , and  $\delta$  are present here. For brevity, in the remaining part of this section we only focus on the use of the arithmetic mean of the radar SINRs.

Next, for one instance included in the top plot of Fig. 1, we visualize the optimized transmit and receive beampatterns of the first subcarrier. The transmit beampattern is defined as in (10), while the radar and user receive beampatterns are  $\|\mathbf{W}_k^H \mathbf{g}_k(\xi)\|^2/T$  and  $\|\mathbf{W}_{k,m}^H \mathbf{g}_{k,m}(\xi)\|^2/T$ , respectively. Fig. 2 depicts the transmit beampattern (black, solid); the vertical lines indicate the locations of the clutter (orange, dashed) and protected directions (red, dash dot), in the top plot, and the locations of the radar target (green, solid) and of the direct (blue, dotted) and indirect (blue, solid) users, in the bottom plot. It is verified by inspection that the transmit beampattern peaks at the target location and has nulls at one clutter and all protected directions. The indirect users are allocated significant power since they require a large SNR to achieve the specified error rate, while it suffices to serve the direct users by sidelobes—the required  $\epsilon = 10^{-5}$  corresponds to  $\text{SNR} \approx 10$  dB for direct users and  $\text{SNR} \approx 40$  dB for indirect users. For the same scenario considered in Fig. 2, Fig. 3 shows (top) the radar receive beampattern with clutter

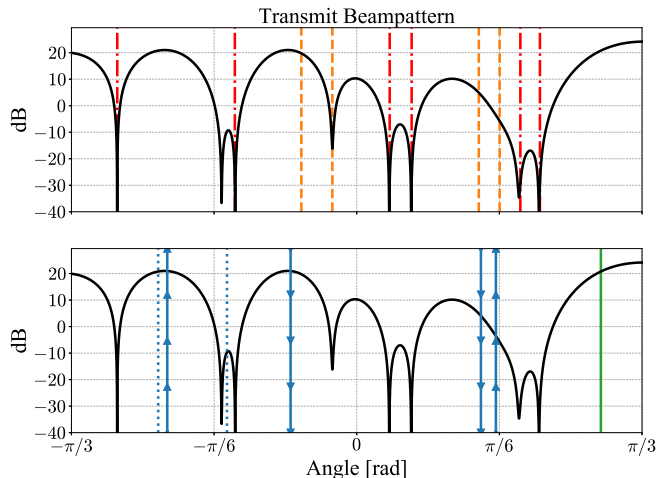


Figure 2. Transmit beampattern (black, solid). In the top plot, the clutter (orange, dashed) and protected (red, dash dot) directions are superimposed. In the bottom plot, the target (green, solid) and user directions are superimposed, including two direct (dotted) and two indirect (solid) users with two indirect paths each. The indirect users are distinguished by the markers.

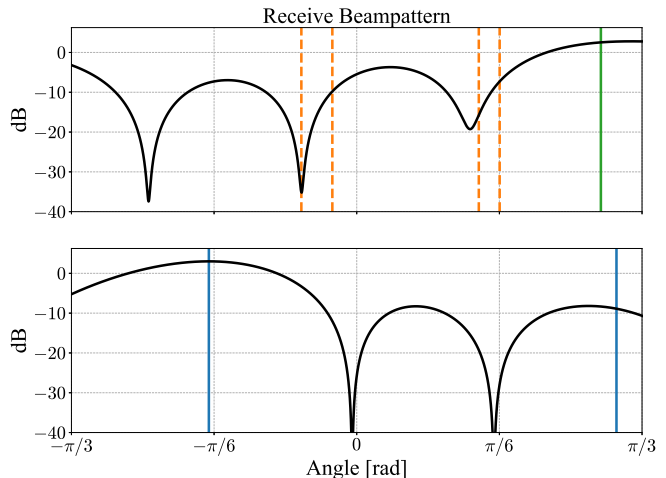


Figure 3. Receive beampatterns for (top) the radar, with target (green, solid) and clutter (orange, dashed) directions superimposed and (bottom) one indirect user with its receive directions superimposed.

and target directions superimposed and (bottom) the receive beampattern of one indirect user with the direction of the received paths superimposed. The radar receive beampattern peaks at the target location and has nulls in two of the clutter directions that were not nulled by the transmit beampattern. The user's beampattern instead emphasizes the two indirect paths.

For another problem instance among those in the top plot of Fig. 1, Fig. 4 illustrates the effect of decreasing  $\epsilon$ , i.e., of shifting priority from the communication users to the radar, on the transmit beampattern obtained in the first subcarrier. Here the line styles match those of Fig. 2. When  $\epsilon = 10^{-2}$  (top), there is a mainlobe centered on the target; instead, when  $\epsilon = 10^{-5}$  (bottom), there are three lobes of similar height directed toward the target and indirect users. Some of the power that was directed toward the radar in the former case has been

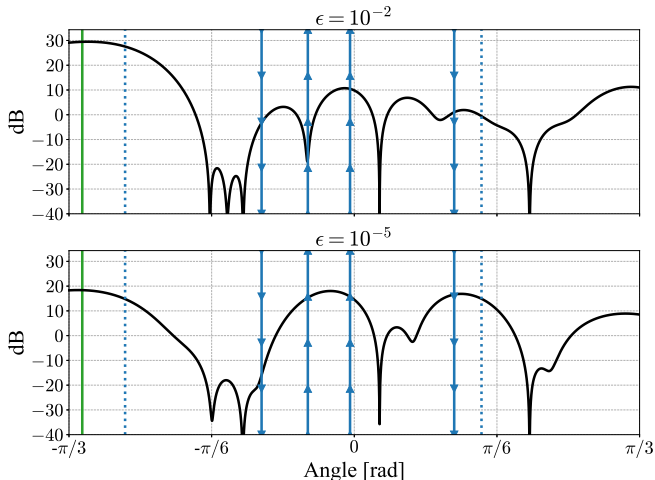


Figure 4. Transmit beampattern (black, solid) for  $\epsilon = 10^{-2}$  (top) and  $\epsilon = 10^{-5}$  (bottom). The target (green, solid) and user directions are superimposed, including two direct (dotted) and two indirect (solid) users with two indirect paths each. The indirect users are distinguished by the markers.

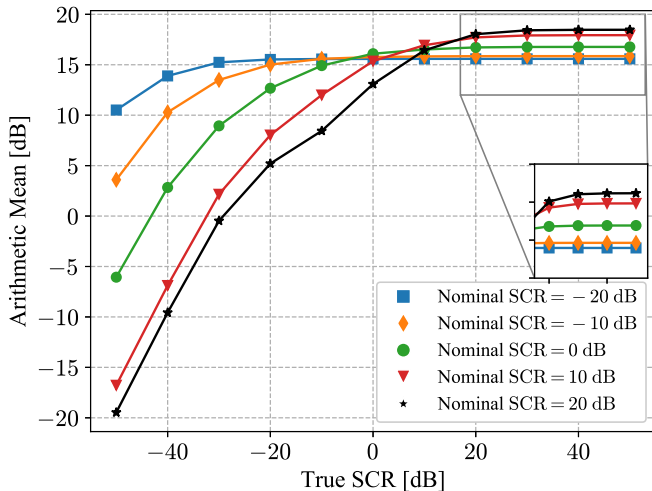


Figure 5. Arithmetic mean of the radar SINRs versus the true SCR, when the system is optimized for an SCR of  $-20$ ,  $-10$ ,  $0$ ,  $10$ , and  $20$  dB.

reallocated to the indirect users in the latter.

We now study the mismatch loss when the true SCR is different from the one employed for design. Fig. 5 reports the arithmetic mean of the radar SINRs versus the true SCR, when the system is optimized for a nominal SCR of  $-20$ ,  $-10$ ,  $0$ ,  $10$ ,  $20$  dB. Evidently, assuming a nominal SCR of  $-20$  dB yields a quite robust design: the optimization prioritizes nulling the clutter directions, thus making the true strength of the clutter less consequential. On the other hand, when the design SCR is  $20$  dB, the objective function decays rapidly as the true SCR decreases, while becoming only slightly favored when the true SCR is  $20$  dB or greater.

Finally, we vary the number of connected users when  $L \in \{0, 2, 4\}$  and  $\delta = 10^{-4}$ . Fig. 6 reports the arithmetic mean of the radar SINRs when there are 4 direct users and  $M$  is increased up to 8 by adding either indirect users (dashed) or direct users (solid). Remarkably, adding indirect users causes

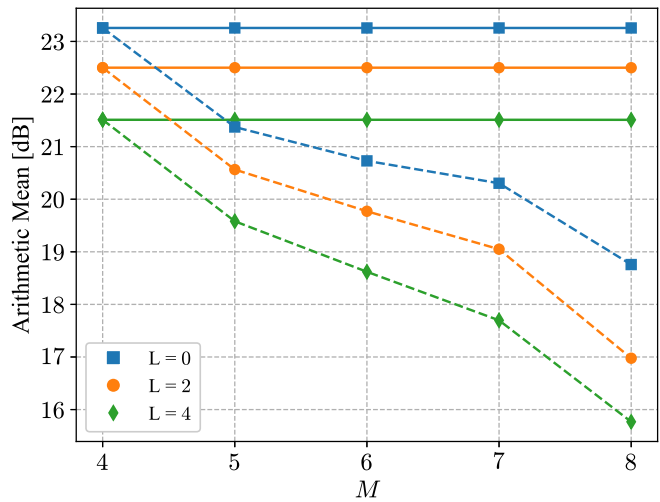


Figure 6. Arithmetic mean of the radar SINRs vs number of users  $M$  for  $L = 0, 2, 4$  and  $\delta = 10^{-4}$ . The solid and dashed lines are generated by adding direct and indirect users, respectively.

a severe performance loss; indeed, for the same error rate, the indirect users requires more physical resources than the direct ones to counteract the channel fading.

## VI. CONCLUSIONS

In this manuscript, we have considered an OFDM-DFRC system employing a DPSK modulation. We have selected the transmit waveforms and the receive filters to maximize the radar performance under constraints on the average radiated power, the error rate of each user, and the beampattern level towards specific directions. The system design results in a non-convex problem, which has been suboptimally solved via an iterative procedure based upon an alternating maximization of the involved variables, a convex restriction of the feasible search set, and the minorization-maximization algorithm. Remarkably, the proposed procedure can be used for a broad family of radar merit functions. The numerical analysis has illustrated the achievable system tradeoffs and the effect of the prior uncertainty on the target strength.

Future developments may consider the sensing of multiple directions on each subcarrier, the use of reconfigurable intelligent surfaces to reach blind spots or create additional indirect paths, and the use of a differential space-time-frequency code to exploit frequency diversity and/or to deliver multiple spatial streams to the users. Also, the optimal system design when a user can simultaneously exploit both direct and indirect signals remains an open problem that requires further investigation.

## APPENDIX

Here we provide the proofs of Propositions 1, 3, 4, and 5.

### A. Proof of Proposition 1

Let  $y = \sum_{i=1}^K \mu_i \gamma(x_i)$ , so that  $f(\mathbf{x}) = \gamma^{-1}(y)$ . Exploiting the formula for the derivative of the inverse function, we have

$$\frac{\partial f(\mathbf{x})}{\partial x_i} = \frac{\mu_i \gamma'(x_i)}{\gamma'(\gamma^{-1}(y))} \quad (49a)$$

$$\frac{\partial^2 f(\mathbf{x})}{\partial x_i^2} = \frac{\mu_i \gamma''(x_i)}{\gamma'(\gamma^{-1}(y))} - \frac{\mu_i^2 [\gamma'(x_i)]^2 \gamma''(\gamma^{-1}(y))}{[\gamma'(\gamma^{-1}(y))]^3} \quad (49b)$$

$$\frac{\partial^2 f(\mathbf{x})}{\partial x_i \partial x_j} = -\frac{\mu_i \mu_j \gamma'(x_i) \gamma'(x_j) \gamma''(\gamma^{-1}(y))}{[\gamma'(\gamma^{-1}(y))]^3} \quad (49c)$$

so that the Hessian matrix is

$$\begin{aligned} \nabla_f^2(\mathbf{x}) &= \frac{1}{\gamma'(\gamma^{-1}(y))} \text{diag}(\{\mu_i \gamma''(x_i)\}) - \frac{\gamma''(\gamma^{-1}(y))}{[\gamma'(\gamma^{-1}(y))]^3} \\ &\quad \times \begin{pmatrix} \mu_1 \gamma'(x_1) \\ \vdots \\ \mu_K \gamma'(x_K) \end{pmatrix} (\mu_1 \gamma'(x_1) \cdots \mu_K \gamma'(x_K)) \end{aligned} \quad (50)$$

that is negative semidefinite for any  $\mathbf{x} \in \bar{\mathbb{R}}^K$  if and only if

$$\begin{aligned} \mathbf{z}^\top \nabla_f^2(\mathbf{x}) \mathbf{z} &= \frac{1}{[\gamma'(\gamma^{-1}(y))]^3} \left( [\gamma'(\gamma^{-1}(y))]^2 \right. \\ &\quad \left. \times \sum_{i=1}^K \mu_i \gamma''(x_i) z_i^2 - \gamma''(\gamma^{-1}(y)) \left( \sum_{i=1}^K \mu_i \gamma'(x_i) z_i \right)^2 \right) \leq 0 \end{aligned} \quad (51)$$

for all  $\mathbf{z} \in \mathbb{R}^K$  and any  $\mathbf{x} \in \bar{\mathbb{R}}^K$ .

In order to prove (51), we follow and generalize the approach in [47, Ch. III, Sec. 16], where the convexity of  $f$  (instead of the concavity) is proven under the condition that  $\gamma \in C^4$  is strictly positive, strictly increasing, and strictly convex. In particular, since either  $\gamma'(x) > 0$  and  $\gamma''(x) < 0$  for all  $x \in \mathbb{R}$ , or  $\gamma'(x) < 0$  and  $\gamma''(x) > 0$  for all  $x \in \mathbb{R}$ , inequality (51) holds if and only if, for any  $\mathbf{x} \in \bar{\mathbb{R}}^K$ ,

$$\frac{[\gamma'(\gamma^{-1}(y))]^2}{|\gamma''(\gamma^{-1}(y))|} \geq \frac{\left( \sum_{i=1}^K \mu_i \gamma'(x_i) z_i \right)^2}{\sum_{i=1}^K \mu_i |\gamma''(x_i)| z_i^2}, \quad \forall \mathbf{z} \in \mathbb{R}^K. \quad (52)$$

Now, by the Cauchy-Schwarz inequality, we have that

$$\begin{aligned} \left( \sum_{i=1}^K \mu_i \gamma'(x_i) z_i \right)^2 &= \left( \sum_{i=1}^K z_i \sqrt{\mu_i |\gamma''(x_i)|} \sqrt{\frac{\mu_i [\gamma'(x_i)]^2}{|\gamma''(x_i)|}} \right)^2 \\ &\leq \sum_{i=1}^K \mu_i |\gamma''(x_i)| z_i^2 \sum_{i=1}^K \mu_i \frac{[\gamma'(x_i)]^2}{|\gamma''(x_i)|} \end{aligned} \quad (53)$$

with equality if and only if  $z_i$  is proportional to  $\frac{\gamma'(x_i)}{|\gamma''(x_i)|}$ . Therefore, condition (52) holds if and only if

$$\frac{[\gamma'(\gamma^{-1}(y))]^2}{|\gamma''(\gamma^{-1}(y))|} \geq \sum_{i=1}^K \mu_i \frac{[\gamma'(x_i)]^2}{|\gamma''(x_i)|}, \quad \forall \mathbf{x} \quad (54)$$

which, upon defining  $g(y) = [\gamma'(\gamma^{-1}(y))]^2 / |\gamma''(\gamma^{-1}(y))|$  and recalling that  $y = \sum_{i=1}^K \mu_i \gamma(x_i)$ , becomes

$$g\left(\sum_{i=1}^K \mu_i \gamma(x_i)\right) \geq \sum_{i=1}^K \mu_i g(x_i), \quad \forall \mathbf{x} \in \bar{\mathbb{R}}^K. \quad (55)$$

This is a concavity condition on  $g$  that, since  $\gamma \in C^4$ , is satisfied if and only if  $g''(y) \leq 0$ , for all  $y$ . Finally, since

$$g'(y) = -\frac{d}{dx} \frac{\gamma'(x)}{\gamma''(x)} \Big|_{x=\gamma^{-1}(y)} - 1 \quad (56a)$$

$$g''(y) = -\frac{1}{\gamma'(x)} \frac{d^2}{dx^2} \frac{\gamma'(x)}{\gamma''(x)} \Big|_{x=\gamma^{-1}(y)} \quad (56b)$$

if  $\gamma'(x) > 0$  and  $\gamma''(x) < 0$  for all  $x \in \bar{\mathbb{R}}$ , and

$$g'(y) = \frac{d}{dx} \frac{\gamma'(x)}{\gamma''(x)} \Big|_{x=\gamma^{-1}(y)} + 1 \quad (57a)$$

$$g''(y) = \frac{1}{\gamma'(x)} \frac{d^2}{dx^2} \frac{\gamma'(x)}{\gamma''(x)} \Big|_{x=\gamma^{-1}(y)} \quad (57b)$$

if  $\gamma'(x) < 0$  and  $\gamma''(x) > 0$  for all  $x \in \bar{\mathbb{R}}$ , we have that  $g$  is concave if and only if  $\gamma'/\gamma''$  is convex.

### B. Proof of Proposition 3

The function  $g$  is twice-differentiable with

$$\nabla_g(\mathbf{u}, x) = \begin{pmatrix} \frac{2}{x} \Psi \mathbf{u} \\ -\frac{1}{x^2} \mathbf{u}^H \Psi \mathbf{u} \end{pmatrix} \quad (58a)$$

$$\nabla_g^2(\mathbf{u}, x) = \frac{2}{x} \begin{pmatrix} \Psi & -\frac{1}{x} \Psi \mathbf{u} \\ -\frac{1}{x} \mathbf{u}^H \Psi & \frac{1}{x^2} \mathbf{u}^H \Psi \mathbf{u} \end{pmatrix}. \quad (58b)$$

Since  $\Psi \succeq 0$  and

$$(\mathbf{I}_N - \Psi \Psi^\dagger) \begin{pmatrix} -\frac{1}{x} \Psi \mathbf{u} \end{pmatrix} = \mathbf{0}_N \quad (59a)$$

$$\frac{1}{x^2} \mathbf{u}^H \Psi \mathbf{u} - \left( \frac{1}{x} \mathbf{u}^H \Psi \right) \Psi^\dagger \begin{pmatrix} \frac{1}{x} \Psi \mathbf{u} \end{pmatrix} = 0 \quad (59b)$$

we conclude that  $\nabla_g^2(\mathbf{u}, x) \succeq 0$  for any  $\mathbf{u} \in \mathbb{C}^N$  and  $x > 0$  [67, Sec. A.5.5], so that  $g$  is convex.

### C. Proof of Proposition 4

The filter  $\mathbf{w}_{k,m}$  only comes into play in C3 and C4. Assume first that  $\kappa_{k,m} = \infty$ . For any feasible  $\mathbf{u}_k$ , the optimal  $\mathbf{w}_{k,m}$  must maximize  $\text{SNR}_{k,m}$  under the constraint set  $\mathcal{W}_{k,m}^d = \{\mathbf{w}_{k,m} \in \mathbb{C}^{TN_m} : \kappa_{k,m} = \infty\}$ . Notice now that

$$\begin{aligned} \max_{\mathbf{w}_{k,m} \in \mathcal{W}_{k,m}^d} \text{SNR}_{k,m} &= \max_{\mathbf{w}_{k,m} \in \mathcal{W}_{k,m}^d} \frac{\mathbf{w}_{k,m}^H \Xi_{k,m} \mathbf{w}_{k,m}}{\|\mathbf{w}_{k,m}\|^2} \\ &= \max_{\mathbf{w}_{k,m} \in \mathcal{W}_{k,m}^d} \frac{\mathbf{w}_{k,m}^H \Xi_{k,m}^d \mathbf{w}_{k,m}}{\|\mathbf{w}_{k,m}\|^2} \leq \lambda_{\max}(\Xi_{k,m}^d). \end{aligned} \quad (60)$$

In the above derivations, the first equality follows from (25), (29), and (45); the second equality is a consequence of the fact that  $(\mathbf{I}_T \otimes \Pi_{k,m}^d) \mathbf{w}_{k,m} = \mathbf{w}_{k,m}$  if  $\mathbf{w}_{k,m} \in \mathcal{W}_{k,m}^d$ ; finally, the last inequality is tight when  $\mathbf{w}_{k,m}$  is proportional to the eigenvector corresponding to the largest eigenvalue of  $\Xi_{k,m}^d$ . The result for  $\kappa_{k,m} = 0$  follows by similar arguments.



#### D. Proof of Proposition 5

Upon solving for the optimal  $\mathbf{w}_{k,m}$  as reported in Proposition 4, the constraint C3 can be reformulated as

$$\begin{cases} \lambda_{\max}(\mathbf{\Xi}_{k,m}^d) \geq \rho_{k,m}^d, & \text{if } \kappa_{k,m} = \infty \\ \lambda_{\max}(\mathbf{\Xi}_{k,m}^i) \geq \rho_{k,m}^i, & \text{if } \kappa_{k,m} = 0 \end{cases}, \quad \forall k, m. \quad (61)$$

If  $\kappa_{k,m} = \infty$ , then we have

$$\begin{aligned} \lambda_{\max}(\mathbf{\Xi}_{k,m}^d) &= \frac{|\beta_{k,m,0}|^2}{\sigma_{z,k,m}^2} \left\| (\mathbf{I}_T \otimes \mathbf{\Pi}_{k,m}^d) \right. \\ &\quad \times \left. (\mathbf{I}_T \otimes \mathbf{g}_{k,m}(\bar{\phi}_{m,0}) \mathbf{s}_k^T(\phi_{m,0})) \mathbf{u}_k \right\|^2 \\ &= \frac{|\beta_{k,m,0}|^2}{\sigma_{z,k,m}^2} \mathbf{g}_{k,m}^H(\bar{\phi}_{m,0}) \mathbf{\Pi}_{k,m}^d \mathbf{g}_{k,m}(\bar{\phi}_{m,0}) \\ &\quad \times \mathbf{u}_k^H (\mathbf{I}_T \otimes \mathbf{s}_k^*(\phi_{m,0}) \mathbf{s}_k^T(\phi_{m,0})) \mathbf{u}_k \\ &= \frac{|\beta_{k,m,0}|^2}{\sigma_{z,k,m}^2} \mathbf{g}_{k,m}^H(\bar{\phi}_{m,0}) \mathbf{\Pi}_{k,m}^d \mathbf{g}_{k,m}(\bar{\phi}_{m,0}) \\ &\quad \times \text{Tr}\{\mathbf{U}_k^H \mathbf{s}_k^*(\phi_{m,0}) \mathbf{s}_k^T(\phi_{m,0}) \mathbf{U}_k\}. \end{aligned} \quad (62)$$

The above derivations show that we must necessarily have  $\mathbf{U}_k^H \mathbf{s}_k^*(\phi_{m,0}) \neq \mathbf{0}_{N_t}$ , as otherwise  $\lambda_{\max}(\mathbf{\Xi}_{k,m}) = 0$ . Also, if  $\text{rank}\{\mathbf{U}_k\} = N_t$ , we can write [69]

$$\begin{aligned} \lambda_{\max}(\mathbf{\Xi}_{k,m}^d) &\geq \frac{N_t |\beta_{k,m,0}|^2}{\sigma_{z,k,m}^2} \lambda_{\min}(\mathbf{U}_k \mathbf{U}_k^H) \\ &\quad \times \mathbf{g}_{k,m}^H(\bar{\phi}_{m,0}) \mathbf{\Pi}_{k,m}^d \mathbf{g}_{k,m}(\bar{\phi}_{m,0}) \end{aligned} \quad (63)$$

and C3 can be satisfied if (46) holds.

If  $\kappa_{k,m} = 0$ , from the Weyl's Theorem [69] we have

$$\begin{aligned} \lambda_{\max}(\mathbf{\Xi}_{k,m}^i) &\leq \sum_{q=1}^{Q_m} \frac{\sigma_{\beta,k,m,q}^2}{\sigma_{z,k,m}^2} \mathbf{g}_{k,m}^H(\bar{\phi}_{m,q}) \mathbf{\Pi}_{k,m}^i \mathbf{g}_{k,m}(\bar{\phi}_{m,q}) \\ &\quad \times \text{Tr}\{\mathbf{U}_k^H \mathbf{s}_k^*(\phi_{m,q}) \mathbf{s}_k^T(\phi_{m,q}) \mathbf{U}_k\} \end{aligned} \quad (64a)$$

$$\begin{aligned} \lambda_{\max}(\mathbf{\Xi}_{k,m}^i) &\geq \max_q \frac{\sigma_{\beta,k,m,q}^2}{\sigma_{z,k,m}^2} \mathbf{g}_{k,m}^H(\bar{\phi}_{m,q}) \mathbf{\Pi}_{k,m}^i \mathbf{g}_{k,m}(\bar{\phi}_{m,q}) \\ &\quad \times \text{Tr}\{\mathbf{U}_k^H \mathbf{s}_k^*(\phi_{m,q}) \mathbf{s}_k^T(\phi_{m,q}) \mathbf{U}_k\}. \end{aligned} \quad (64b)$$

The above inequalities show that we must necessarily have  $\mathbf{U}_k^H \mathbf{s}_k^*(\phi_{m,q}) \neq \mathbf{0}_{N_t}$  for at least one indirect path  $q \in \{1, \dots, Q_m\}$ . Also, if  $\text{rank}\{\mathbf{U}_k\} = N_t$ , we can write [69]

$$\begin{aligned} \lambda_{\max}(\mathbf{\Xi}_{k,m}^i) &\geq \max_q \frac{N_t \sigma_{\beta,k,m,q}^2}{\sigma_{z,k,m}^2} \lambda_{\min}(\mathbf{U}_k \mathbf{U}_k^H) \\ &\quad \times \mathbf{g}_{k,m}^H(\bar{\phi}_{m,q}) \mathbf{\Pi}_{k,m}^i \mathbf{g}_{k,m}(\bar{\phi}_{m,q}) \end{aligned} \quad (65)$$

and C3 can be satisfied if (46) holds.

#### REFERENCES

- [1] H. Griffiths *et al.*, "Radar spectrum engineering and management: Technical and regulatory issues," *Proceedings of the IEEE*, vol. 103, no. 1, pp. 85–102, Jan. 2015.
- [2] H. Mazar, *Radio spectrum Management: Policies, regulations and techniques*. USA: John Wiley & Sons, 2016.
- [3] V. Sridhar and R. Prasad, "Analysis of spectrum pricing for commercial mobile services: A cross country study," *Telecommunications Policy*, 2021.
- [4] N. Devroye, M. Vu, and V. Tarokh, "Cognitive radio networks," *IEEE Signal Processing Magazine*, vol. 25, no. 6, pp. 12–23, Nov. 2008.
- [5] J. Proakis and M. Salehi, *Digital Communications*, 5th ed. New York, NY, USA: McGraw-Hill Higher Education, 2014.
- [6] L. Dai *et al.*, "A survey of non-orthogonal multiple access for 5G," *IEEE Communications Surveys Tutorials*, vol. 20, no. 3, pp. 2294–2323, thirdquarter 2018.
- [7] L. Venturino, N. Prasad, and X. Wang, "Coordinated scheduling and power allocation in downlink multicell OFDMA networks," *IEEE Transactions on Vehicular Technology*, vol. 58, no. 6, pp. 2835–2848, Jul. 2009.
- [8] H. Zhang *et al.*, "Weighted sum-rate maximization in multi-cell networks via coordinated scheduling and discrete power control," *IEEE Journal on Selected Areas in Communications*, vol. 29, no. 6, pp. 1214–1224, Jun. 2011.
- [9] E. Björnson and L. Sanguinetti, "Scalable cell-free massive MIMO systems," *IEEE Transactions on Communications*, vol. 68, no. 7, pp. 4247–4261, Jul. 2020.
- [10] L. Venturino, N. Prasad, X. Wang, and M. Madhian, "Design of linear dispersion codes for practical MIMO-OFDM systems," *IEEE Journal of Selected Topics in Signal Processing*, vol. 1, no. 1, pp. 178–188, Jun. 2007.
- [11] N. Fatema, G. Hua, Y. Xiang, D. Peng, and I. Natgunanathan, "Massive MIMO linear precoding: A survey," *IEEE Systems Journal*, vol. 12, no. 4, pp. 3920–3931, Dec. 2018.
- [12] M. A. Albreem, M. Juntti, and S. Shahabuddin, "Massive MIMO detection techniques: A survey," *IEEE Communications Surveys Tutorials*, vol. 21, no. 4, pp. 3109–3132, Fourthquarter 2019.
- [13] S. H. Javadi and A. Farina, "Radar networks: A review of features and challenges," *Information Fusion*, vol. 61, pp. 48–55, 2020.
- [14] S. Miranda, C. Baker, K. Woodbridge, and H. Griffiths, "Knowledge-based resource management for multifunction radar: a look at scheduling and task prioritization," *IEEE Signal Processing Magazine*, vol. 23, no. 1, pp. 66–76, Jan. 2006.
- [15] S. Haykin, "Cognitive radar: a way of the future," *IEEE Signal Processing Magazine*, vol. 23, no. 1, pp. 30–40, Jan. 2006.
- [16] S. Z. Gurbuz *et al.*, "An overview of cognitive radar: Past, present, and future," *IEEE Aerospace and Electronic Systems Magazine*, vol. 34, no. 12, pp. 6–18, Dec. 2019.
- [17] J. Li and P. Stoica, *MIMO radar signal processing*. Hoboken, USA: John Wiley & Sons, 2009.
- [18] S. D. Blunt and E. L. Mokole, "Overview of radar waveform diversity," *IEEE Aerospace and Electronic Systems Magazine*, vol. 31, no. 11, pp. 2–42, Nov. 2016.
- [19] E. Grossi, M. Lops, and L. Venturino, "Robust waveform design for MIMO radars," *IEEE Transactions on Signal Processing*, vol. 59, no. 7, pp. 3262–3271, Jul. 2011.
- [20] E. Grossi, M. Lops, and L. Venturino, "Min–max waveform design for MIMO radars under unknown correlation of the target scattering," *Signal Processing*, vol. 92, no. 6, pp. 1550–1558, 2012.
- [21] W. Roberts, P. Stoica, J. Li, T. Yardibi, and F. A. Sadjadi, "Iterative adaptive approaches to MIMO radar imaging," *IEEE Journal of Selected Topics in Signal Processing*, vol. 4, no. 1, pp. 5–20, Feb 2010.
- [22] J. Liu and J. Li, "Robust detection in MIMO radar with steering vector mismatches," *IEEE Transactions on Signal Processing*, vol. 67, no. 20, pp. 5270–5280, Oct. 2019.
- [23] K. Alhujaili, V. Monga, and M. Rangaswamy, "Transmit MIMO radar beam pattern design via optimization on the complex circle manifold," *IEEE Transactions on Signal Processing*, vol. 67, no. 13, pp. 3561–3575, Jul. 2019.
- [24] X. Yu, G. Cui, J. Yang, L. Kong, and J. Li, "Wideband MIMO radar waveform design," *IEEE Transactions on Signal Processing*, vol. 67, no. 13, pp. 3487–3501, Jul. 2019.
- [25] L. Zheng, M. Lops, Y. C. Eldar, and X. Wang, "Radar and communication coexistence: An overview: A review of recent methods," *IEEE Signal Processing Magazine*, vol. 36, no. 5, pp. 85–99, Sep. 2019.
- [26] F. Liu, C. Masouros, A. Petropulu, H. Griffiths, and L. Hanzo, "Joint radar and communication design: Applications, state-of-the-art, and the road ahead," *IEEE Transactions on Communications*, vol. 68, no. 6, pp. 3834 – 3862, Jun. 2020.
- [27] A. Martone and M. Amin, "A view on radar and communication systems coexistence and dual functionality in the era of spectrum sensing," *Digital Signal Processing*, p. 103135, 2021.
- [28] N. C. Luong, X. Lu, D. T. Hoang, D. Niyato, and D. I. Kim, "Radio resource management in joint radar and communication: A comprehensive survey," *IEEE Communications Surveys Tutorials*, vol. 23, no. 2, pp. 780–814, 2021.
- [29] F. Wang, H. Li, and M. A. Govoni, "Power allocation and co-design of multicarrier communication and radar systems for spectral coexistence," *IEEE Transactions on Signal Processing*, vol. 67, no. 14, pp. 3818–3831, Jul. 2019.

- [30] Z. Cheng, B. Liao, S. Shi, Z. He, and J. Li, "Co-design for overlaid MIMO radar and downlink MISO communication systems via Cramér-Rao bound minimization," *IEEE Transactions on Signal Processing*, vol. 67, no. 24, pp. 6227–6240, Dec. 2019.
- [31] E. Grossi, M. Lops, and L. Venturino, "Joint design of surveillance radar and MIMO communication in cluttered environments," *IEEE Transactions on Signal Processing*, vol. 68, pp. 1544–1557, 2020.
- [32] E. Grossi, M. Lops, and L. Venturino, "Energy efficiency optimization in radar-communication spectrum sharing," *IEEE Transactions on Signal Processing*, vol. 69, pp. 3541–3554, 2021.
- [33] J. Qian, L. Venturino, M. Lops, and X. Wang, "Harmonic mean SINR maximization in a cognitive radar with communication spectrum sharing," in *2021 IEEE Radar Conference (RadarConf21)*, May 2021, pp. 1–6.
- [34] E. Grossi, M. Lops, and L. Venturino, "Adaptive detection and localization exploiting the IEEE 802.11ad standard," *IEEE Transactions on Wireless Communications*, vol. 19, no. 7, pp. 4394–4407, Jul. 2020.
- [35] E. Grossi, M. Lops, A. M. Tulino, and L. Venturino, "Opportunistic sensing using mmwave communication signals: A subspace approach," *IEEE Transactions on Wireless Communications*, vol. 20, no. 7, pp. 4420–4434, Jul. 2021.
- [36] R. M. Mealey, "A method for calculating error probabilities in a radar communication system," *IEEE Transactions on Space Electronics and Telemetry*, vol. 9, no. 2, pp. 37–42, Jun. 1963.
- [37] S. D. Blunt, M. R. Cook, and J. Stiles, "Embedding information into radar emissions via waveform implementation," in *2010 International Waveform Diversity and Design Conference*, Aug. 2010, pp. 195–199.
- [38] A. Hassanien, M. G. Amin, Y. D. Zhang, and F. Ahmad, "Signaling strategies for dual-function radar communications: an overview," *IEEE Aerospace and Electronic Systems Magazine*, vol. 31, no. 10, pp. 36–45, Oct. 2016.
- [39] M. Nowak, M. Wicks, Z. Zhang, and Z. Wu, "Co-designed radar-communication using linear frequency modulation waveform," *IEEE Aerospace and Electronic Systems Magazine*, vol. 31, no. 10, pp. 28–35, Oct. 2016.
- [40] A. Ahmed, Y. D. Zhang, and Y. Gu, "Dual-function radar-communications using QAM-based sidelobe modulation," *Digital Signal Processing*, vol. 82, pp. 166–174, 2018.
- [41] T. Huang, N. Shlezinger, X. Xu, Y. Liu, and Y. C. Eldar, "MAJoRCom: A dual-function radar communication system using index modulation," *IEEE Transactions on Signal Processing*, vol. 68, pp. 3423–3438, 2020.
- [42] A. Ahmed, Y. D. Zhang, A. Hassanien, and B. Himed, "OFDM-based joint radar-communication system: Optimal sub-carrier allocation and power distribution by exploiting mutual information," in *2019 53rd Asilomar Conference on Signals, Systems, and Computers*, Nov. 2019, pp. 559–563.
- [43] C. Shi, Y. Wang, F. Wang, S. Salous, and J. Zhou, "Joint optimization scheme for subcarrier selection and power allocation in multicarrier dual-function radar-communication system," *IEEE Systems Journal*, vol. 15, no. 1, pp. 947–958, Mar. 2021.
- [44] M. Bică and V. Koivunen, "Multicarrier radar-communications waveform design for RF convergence and coexistence," in *ICASSP 2019 - 2019 IEEE International Conference on Acoustics, Speech and Signal Processing (ICASSP)*, May 2019, pp. 7780–7784.
- [45] M. F. Keskin, V. Koivunen, and H. Wymeersch, "Limited feedforward waveform design for OFDM dual-functional radar-communications," *IEEE Transactions on Signal Processing*, vol. 69, pp. 2955–2970, 2021.
- [46] M. Temiz, E. Alsusa, and M. W. Baidas, "Optimized precoders for massive MIMO OFDM dual radar-communication systems," *IEEE Transactions on Communications*, vol. 69, no. 7, pp. 4781–4794, Jul. 2021.
- [47] G. H. Hardy, J. E. Littlewood, and G. Pólya, *Inequalities*. Cambridge, UK: Cambridge University Press, 1934.
- [48] P. Bullen, *Handbook of Means and Their Inequalities*, ser. Mathematics and Its Applications. Netherlands: Springer, 2003.
- [49] H. Lee and S. Kim, "Muirhead's and Holland's inequalities of mixed power means for positive real numbers," *Journal of applied mathematics & informatics*, vol. 35, no. 1-2, p. 33–44, Jan. 2017.
- [50] M. R. Bell, "Information theory and radar waveform design," *IEEE Transactions on Information Theory*, vol. 39, no. 5, pp. 1578–1597, Sep. 1993.
- [51] Y. Yang and R. S. Blum, "MIMO radar waveform design based on mutual information and minimum mean-square error estimation," *IEEE Transactions on Aerospace and Electronic Systems*, vol. 43, no. 1, pp. 330–343, Jan. 2007.
- [52] A. De Maio, M. Lops, and L. Venturino, "Diversity-integration tradeoffs in MIMO detection," *IEEE Transactions on Signal Processing*, vol. 56, no. 10, pp. 5051–5061, Oct. 2008.
- [53] S. Sen and A. Nehorai, "OFDM MIMO radar with mutual-information waveform design for low-grazing angle tracking," *IEEE Transactions on Signal Processing*, vol. 58, no. 6, pp. 3152–3162, Jun. 2010.
- [54] A. Aubry, M. Lops, A. M. Tulino, and L. Venturino, "On MIMO detection under non-Gaussian target scattering," *IEEE Transactions on Information Theory*, vol. 56, no. 11, pp. 5822–5838, Nov. 2010.
- [55] G. H. Jajamovich, M. Lops, and X. Wang, "Space-time coding for mimo radar detection and ranging," *IEEE Transactions on Signal Processing*, vol. 58, no. 12, pp. 6195–6206, Dec. 2010.
- [56] M. A. Richards, *Fundamentals of radar signal processing*. New York, NY, USA: McGraw-Hill, 2005.
- [57] E. Grossi and M. Lops, "Space-time code design for MIMO detection based on Kullback-Leibler divergence," *IEEE Transactions on Information Theory*, vol. 58, no. 6, pp. 3989–4004, 2012.
- [58] C. Sturm and W. Wiesbeck, "Waveform design and signal processing aspects for fusion of wireless communications and radar sensing," *Proceedings of the IEEE*, vol. 99, no. 7, pp. 1236–1259, Jul. 2011.
- [59] K. M. Braun, "OFDM radar algorithms in mobile communication networks," Ph.D. dissertation, Karlsruhe Institute of Technology (KIT), 2014.
- [60] M. Bică and V. Koivunen, "Generalized multicarrier radar: Models and performance," *IEEE Transactions on Signal Processing*, vol. 64, no. 17, pp. 4389–4402, Sep. 2016.
- [61] M. I. Skolnik, *Introduction to radar systems*, 3rd ed., ser. McGraw-Hill international editions. Electrical engineering series. Boston, MA, USA: McGraw-Hill, 2001.
- [62] J. A. Roberts and J. M. Bargallo, "DPSK performance for indoor wireless Rician fading channels," *IEEE Transactions on Communications*, vol. 42, no. 234, pp. 592–596, 1994.
- [63] S. Jonqyin and I. S. Reed, "Performance of MDPSK, MPSK, and non-coherent MFSK in wireless Rician fading channels," *IEEE Transactions on Communications*, vol. 47, no. 6, pp. 813–816, Jun. 1999.
- [64] K. Lange, "A tutorial on MM algorithms," *The American Statistician*, vol. 58, no. 1, p. 30–37, Feb. 2004.
- [65] B. C. Rennie, "Exponential means," *James Cook Mathematical Notes*, vol. 6, no. 54, pp. 6023–6024, Feb. 1991.
- [66] C. K. Paww and D. L. Schilling, "Probability of error of  $M$ -ary PSK and DPSK on a Rayleigh fading channel," *IEEE Transactions on Communications*, vol. 36, no. 6, pp. 755–756, 1988.
- [67] S. Boyd, S. P. Boyd, and L. Vandenberghe, *Convex optimization*. Cambridge, United Kingdom: Cambridge University Press, 2004.
- [68] N. Sidiropoulos, T. Davidson, and Z.-Q. Luo, "Transmit beamforming for physical-layer multicasting," *IEEE Transactions on Signal Processing*, vol. 54, no. 6, pp. 2239–2251, 2006.
- [69] R. A. Horn and C. R. Johnson, *Matrix Analysis*, 2nd ed. USA: Cambridge University Press, 2012.